

Composably-secure data-processing in continuous variable quantum key distribution

Alexander G. Mountogiannakis¹, Panagiotis Papanastasiou¹, Boris Braverman², and Stefano Pirandola¹

¹*Department of Computer Science, University of York, York YO10 5GH, UK*

²*Xanadu, 372 Richmond St W, Toronto, M5V 2L7, Canada*

Continuous-variable quantum key distribution employs the quadratures of a bosonic mode to establish a secret key between two remote parties. The resulting secret-key rate depends not only on the loss and noise in the communication channel, but also on a series of data-processing steps that are needed for transforming shared correlations into a final string of secret bits. Within the general setting of composable finite-size security, we consider a coherent-state protocol, whose quantum communication is simulated and classical data is post-processed via procedures of parameter estimation, error correction and privacy amplification. Such steps are presented in detail and suitably adapted to follow recently-developed tools for composable security analysis. For this advanced approach on data-processing, we provide a Python-based environment that allows us to investigate and optimize the protocol parameters to be used in practical experimental implementations.

I. INTRODUCTION

A quantum key distribution (QKD) protocol involves two distant authenticated parties (Alice and Bob), whose aim is to establish a secret key by communicating over a potentially insecure quantum channel [1]. The security of QKD is derived from the laws of quantum mechanics, namely the uncertainty principle or the no-cloning theorem. In 1984, Bennett and Brassard introduced the first QKD protocol [2], in which information is encoded on a property of a discrete-variable (DV) system, such as the polarization of a photon. This class of protocols started the area of DV-QKD and their security has been extensively studied, recently at the composable level with automated optimizations [3].

Later on, at the beginning of the 2000s, another more modern family of protocols emerged, in which information is encoded in the position and momentum quadratures of a bosonic mode [4, 5]. These continuous-variable (CV) QKD protocols are particularly practical and cost-effective, being already compatible with the current telecommunication technology [1, 6]. CV-QKD protocols are very suitable to reach high rates of communication (e.g., comparable with the ultimate channel limits [7]) over distances that are compatible with metropolitan areas [8]. Recently, CV-QKD protocols have also been shown to reach very long distances comparable to those of DV protocols [9, 10].

In a basic CV-QKD protocol, Alice encodes a classical variable in the coherent states of a bosonic mode via Gaussian modulation. These states are then transmitted to Bob via the noisy communication channel. At the output, Bob measures the received states via homodyne [4, 9] (or heterodyne [5]) detection in order to decode Alice's encoded information. In the worst-case scenario, all the loss and noise present in the channel is ascribed to a malicious party (Eve) who tries to intercept the states and obtain information about the key. By carefully estimating Eve's perturbation, Alice and Bob can apply procedures of error correction (EC) to remove noise from their data, and then privacy amplification (PA), which

makes their error-corrected data completely secret, i.e., decoupled from Eve.

In this work, we consider the basic CV-QKD protocol based on Gaussian modulation of coherent states and homodyne detection (even though our approach can be readily extended to considering heterodyne detection and other types of CV-QKD protocols). Starting from a simulation of the quantum communication in noisy conditions, we process the generated data into a finite-size secret key which is composable secure against collective Gaussian attacks. Besides developing the technical procedure step-by-step, we implement it completely in the open-access Python library (CVQKDsim) associated with this research paper [11]. In particular, our procedure for data processing matches the composable secret key rate recently developed in Ref. [12], valid for both free-space and fiber-based communication links.

In order to address a short-range regime with relatively-high values of the signal to noise ratio (SNR), the step of EC is based on high-rate (non-binary) low-density parity check codes (LDPC) [13–17], whose decoding is performed by means of a suitable iterative sum-product algorithm [14, 18] (even though the min-sum algorithm [19] can be used as an alternative). After EC, the procedure of PA is based on universal hash functions [20]. Because of the length of the generated strings can be substantial, techniques with low complexity are preferred, so that we use the Toeplitz-based hash function, which is simple, parallelizable and can moreover be accelerated by using the Fast Fourier Transform (FFT) [21].

The paper is structured as follows. In Sec. II we start with the description of the coherent state protocol assuming a realistic model for the detector setup. After an initial analysis of its asymptotic security, we discuss the steps of parameter estimation (PE), EC and PA, ending with the composable secret key rate of the protocol. In Sec. III, we go into further details of the protocol simulation and data processing, also presenting the pseudocode for the entire process. In Sec. IV we provide numerical results that are obtained by our Python library in simulated experiments. Finally, Sec. V is for conclusions.

II. COHERENT-STATE PROTOCOL AND SECURITY ANALYSIS

A. General description and mutual information

In a coherent-state protocol [1, Sec. 7], Alice prepares a bosonic mode A in a coherent state $|\alpha\rangle$ whose amplitude is Gaussian-modulated (see Fig. 1 for a schematic). In other words, we may write $\alpha = (q + ip)/2$, where $x = q, p$ is the mean value of the generic quadrature $\hat{x} = \hat{q}, \hat{p}$, which is randomly chosen according to a zero-mean Gaussian distribution $\mathcal{N}(0, \sigma_x^2)$ with variance $\sigma_x^2 := \mu - 1 \geq 0$, i.e., according to the Gaussian probability density

$$p_{\mathcal{N}}(x) = (\sqrt{2\pi}\sigma_x)^{-1} \exp[-x^2/(2\sigma_x^2)]. \quad (1)$$

Note that we have $q = 2 \operatorname{Re} \alpha$ and $p = 2 \operatorname{Im} \alpha$ (in fact, we use the notation of Ref. [6, Sec. II], where $[\hat{q}, \hat{p}] = 2i$ and the vacuum state has noise-variance equal to 1).

The coherent state is sent through an optical fiber of length L which can be modelled as a thermal-loss channel with transmissivity $T = 10^{-\frac{AL}{10}}$ (e.g., $A = 0.2$ dB/km) and thermal noise $\omega = 2\bar{n} + 1$, where \bar{n} is the thermal number associated with an environmental mode E . The process can equivalently be represented by a beam-splitter with transmissivity T mixing Alice's mode A with mode E , which is in a thermal state with \bar{n} mean photons. The environmental thermal state can be purified in a two-mode squeezed vacuum state (TMSV) Φ_{eE} , i.e., a Gaussian state for modes e and E , with zero mean and covariance matrix (CM) [6]

$$\mathbf{V}_{eE}(\omega) = \begin{pmatrix} \omega \mathbf{I} & \sqrt{\omega^2 - 1} \mathbf{Z} \\ \sqrt{\omega^2 - 1} \mathbf{Z} & \omega \mathbf{I} \end{pmatrix}, \quad (2)$$

where $\mathbf{I} := \operatorname{diag}(1, 1)$ and $\mathbf{Z} := \operatorname{diag}(1, -1)$. This dilation, where Eve uses a beam splitter and a TMSV state, is known as an “entangling cloner” attack and represents the fundamental interaction of a realistic collective Gaussian attack [22] (see Fig. 1).

At the other end of the channel, Bob measures the incoming state using a homodyne detector with quantum efficiency η and electronic noise v_{el} , which is randomly switched between the two quadratures (we may also include local coupling losses in parameter η). Let us denote by \hat{y} the generic quadrature of Bob's mode B just before the (ideal) homodyne detector. Then, the outcome y of the detector satisfies the input-output formula

$$y = \sqrt{T\eta}x + z, \quad (3)$$

where z is (or approximately is) a Gaussian noise variable with zero mean and variance

$$\sigma_z^2 = 1 + v_{\text{el}} + \eta T \xi, \quad (4)$$

where v_{el} is the electronic noise of the setup and ξ is channel excess noise, defined by

$$\xi := \frac{1 - T}{T}(\omega - 1). \quad (5)$$

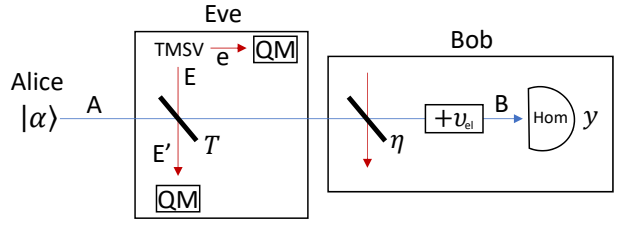


FIG. 1: Structure of the CV-QKD protocol with coherent states considering a receiver that might have trusted levels of inefficiency and electronic noise. In the middle, the thermal-loss channel is induced by the collective Gaussian attack of Eve, who uses a beam-splitter with transmissivity T and a TMSV state with variance ω . Eve's output are stored in quantum memories (QM) for a later optimized quantum measurement bounded by the Holevo information.

Here it is important to make two observations. The first consideration is about the general treatment of the detector at Bob's side, where we assume the potential presence of trusted levels of quantum efficiency and electronic noise. In the worst case scenario, these levels can be put equal to zero and assume that these contributions are implicitly part of the channel transmissivity and excess noise. In other words, one has $T\eta \rightarrow T$ in Eq. (3), while v_{el} becomes part of ξ in Eq. (4), so that $\xi \rightarrow \xi + v_{\text{el}}/T$ in Eq. (5). The second point is that there might be other imperfections in Alice's and Bob's setups that are not mitigated or controllable by the parties (e.g., modulation and phase noise). These imperfections are automatically included in the channel loss and noise via the general relations of Eq. (3) and (4). Furthermore, the extra noise contributions can be considered to be Gaussian in the worst-case scenario, resorting to the optimality of Gaussian attacks in CV-QKD [1].

Assuming the general scenario in Fig. 1, let us compute Alice and Bob's mutual information. From Eq. (3), we compute the variance of y , which is equal to

$$\begin{aligned} \sigma_y^2 &= T\eta\sigma_x^2 + \sigma_z^2 \\ &= T\eta(\mu - 1 + \xi) + 1 + v_{\text{el}}. \end{aligned} \quad (6)$$

For the conditional variance, we compute

$$\sigma_{y|x}^2 = \sigma_y^2(\mu = 1) = \eta T \xi + 1 + v_{\text{el}}. \quad (7)$$

The mutual information associated with the CVs x and y is given by the difference between the differential entropy $h(y)$ of y and the conditional entropy $h(y|x)$, i.e.,

$$I(x : y) = h(y) - h(y|x) = \frac{1}{2} \log_2 \left(\frac{\sigma_y^2}{\sigma_{y|x}^2} \right) \quad (8)$$

$$= \frac{1}{2} \log_2 \left[1 + \frac{\mu - 1}{\xi + (1 + v_{\text{el}})/T\eta} \right] \quad (9)$$

$$= \frac{1}{2} \log_2 [1 + \text{SNR}]. \quad (10)$$

The mutual information has the same value no matter if it is computed in direct reconciliation (DR), where Bob infers Alice's variable, or in reverse reconciliation (RR), where Alice infers Bob's variable.

As we can see from the expression above, the mutual information contains the signal-to-noise (SNR) term

$$\text{SNR} = (\mu - 1)/\mathcal{X}, \quad (11)$$

where

$$\mathcal{X} = \xi + (1 + v_{\text{el}})/T\eta \quad (12)$$

is the equivalent noise. The joint Gaussian distribution of the two variables x and y has zero mean and CM

$$\Sigma_{xy} = \begin{pmatrix} \sigma_x^2 & \rho\sigma_x\sigma_y \\ \rho\sigma_x\sigma_y & \sigma_y^2 \end{pmatrix} \quad (13)$$

where $\rho = \mathbb{E}(xy)/\sigma_x\sigma_y$ is a correlation parameter. From the classical formula $I(x : y) = -\log_2(1 - \rho^2)$ [23], we see that

$$\rho = \sqrt{\frac{\text{SNR}}{1 + \text{SNR}}}. \quad (14)$$

It is important to stress that, in order to asymptotically achieve the maximum number of shared bits $I(x : y)$ per channel use, in RR Bob needs to send $h(y|x)$ bits through the public channel according to Slepian-Wolf coding [24, 25]. In practice, Alice and Bob will perform a sub-optimal procedure of EC/reconciliation revealing more information $\text{leak}_{\text{EC}} \geq h(y|x)$. In order to account for this, one assumes that only a portion $\beta I(x : y)$ of the mutual information can be achieved by using the reconciliation parameter $\beta \in [0, 1]$.

In the ideal case of $\beta = 1$, the mutual information between the parties depends monotonically on the SNR. However, in a realistic case where the reconciliation is not efficient ($\beta < 1$), the extra leaked information $(1 - \beta)I(x : y)$ also depends on the SNR. Therefore, by trying to balance the terms $\beta I(x : y)$ and $\text{leak}_{\text{EC}} = h(y|x) + (1 - \beta)I(x : y)$, one finds an optimal value for the SNR and, therefore, an optimal value for the Gaussian modulation μ . In practice, this optimal working point can be precisely computed only after T and ξ are estimated through the procedure of PE (which is discussed later in Sec. II C). However, a rough estimate of this optimal value can be obtained by an educated guess of the channel parameters (e.g., the approximate transmissivity could be guessed from the length of the fiber and the expected standard loss rate).

B. Asymptotic key rate

Let us compute the secret key rate that the parties would be able to achieve if they could use the quantum communication channel an infinite number of times. Besides $\beta I(x : y)$, we need to calculate Eve's Holevo information $\chi(E : y)$ on Bob's outcome y . This is in fact

the maximum information that Eve can steal under the assumption of collective attacks, where she perturbs the channel in an independent and identical way while storing all her outputs in a quantum memory (to be optimally measured at the end of the protocol). It is important to stress that, for any processing done by Bob $y \rightarrow y'$, we have $\chi(E : y') \leq \chi(E : y)$ so that the latter value can always be taken as an upper bound for the actual eavesdropping performance.

Let us introduce the entanglement-based representation of the protocol, where Alice's input ensemble of coherent states is generated on mode A by heterodyning mode A' of a TMSV $\Phi_{A'A}$ with variance μ . Note that this representation is not strictly necessary in our analysis (which may be carried over in prepare and measure completely), but we adopt it anyway for completeness, so as to give the total state with all the correlations between Alice, Bob and Eve.

The output modes A' and B shared by the parties will be in a zero-mean Gaussian state $\rho_{A'B}$ with CM [6]

$$\mathbf{V}_{A'B} = \begin{pmatrix} \mu\mathbf{I} & c\mathbf{Z} \\ c\mathbf{Z} & b\mathbf{I} \end{pmatrix}, \quad (15)$$

where we have set

$$c := \sqrt{T\eta(\mu^2 - 1)}, \quad (16)$$

$$b := T\eta(\mu + \xi) + 1 - T\eta + v_{\text{el}}. \quad (17)$$

Then, the global output state $\rho_{A'BeE'}$ of Alice, Bob and Eve is zero-mean Gaussian with CM

$$\mathbf{V}_{A'BeE'} = \begin{pmatrix} \mu\mathbf{I} & c\mathbf{Z} & \mathbf{0} & \zeta\mathbf{Z} \\ c\mathbf{Z} & b\mathbf{I} & \gamma\mathbf{Z} & \theta\mathbf{I} \\ \mathbf{0} & \gamma\mathbf{Z} & \omega\mathbf{I} & \psi\mathbf{Z} \\ \zeta\mathbf{Z} & \theta\mathbf{I} & \psi\mathbf{Z} & \phi\mathbf{I} \end{pmatrix}, \quad (18)$$

where $\mathbf{0}$ is the 2×2 zero matrix and we set

$$\gamma := \sqrt{\eta(1 - T)(\omega^2 - 1)}, \quad (19)$$

$$\zeta := -\sqrt{(1 - T)(\mu^2 - 1)}, \quad (20)$$

$$\theta := \sqrt{\eta T(1 - T)}(\omega - \mu), \quad (21)$$

$$\psi = \sqrt{T(\omega^2 - 1)}, \quad (22)$$

$$\phi := T\omega + (1 - T)\mu. \quad (23)$$

To compute the Holevo bound, we need to derive the von Neumann entropies $S(\rho_{eE'})$ and $S(\rho_{eE'|y})$ which can be computed from the symplectic spectra of the reduced CM $\mathbf{V}_{eE'}$ and the conditional CM $\mathbf{V}_{eE'|y}$. Setting

$$\mathbf{C} = \begin{pmatrix} \gamma\mathbf{Z} & \theta\mathbf{I} \end{pmatrix}, \quad \mathbf{\Pi} := \begin{pmatrix} 1 & 0 \\ 0 & 0 \end{pmatrix}, \quad (24)$$

we may use the pseudo-inverse to compute [6]

$$\mathbf{V}_{eE'|y} = \mathbf{V}_{eE'} - \mathbf{C}^T [\mathbf{\Pi}(b\mathbf{I})\mathbf{\Pi}]^{-1} \mathbf{C} \quad (25)$$

$$= \mathbf{V}_{eE'} - b^{-1} \mathbf{C}^T \mathbf{\Pi} \mathbf{C} \quad (26)$$

$$= \begin{pmatrix} \omega\mathbf{I} & \psi\mathbf{Z} \\ \psi\mathbf{Z} & \phi\mathbf{I} \end{pmatrix} - b^{-1} \begin{pmatrix} \gamma^2\mathbf{\Pi} & \gamma\theta\mathbf{\Pi} \\ \gamma\theta\mathbf{\Pi} & \theta^2\mathbf{\Pi} \end{pmatrix}. \quad (27)$$

Since both $\mathbf{V}_{eE'}$ and $\mathbf{V}_{eE'|y}$ are two-mode CMs, it is easy to compute their symplectic spectra, that we denote by $\{\nu_{\pm}\}$ and $\{\tilde{\nu}_{\pm}\}$, respectively. Their general analytical expressions are too cumbersome to show here unless we take the high-modulation limit $\mu \gg 1$. For instance, we have $\nu_+ \rightarrow (1 - T)\mu$ and $\nu_- \rightarrow \omega$.

Finally, we may write the Holevo bound as

$$\begin{aligned}\chi(E : y) &= S(\rho_{eE'}) - S(\rho_{eE'|y}) \\ &= h(\nu_+) + h(\nu_-) - h(\tilde{\nu}_+) - h(\tilde{\nu}_-),\end{aligned}\quad (28)$$

where

$$h(\nu) := \frac{\nu + 1}{2} \log_2 \frac{\nu + 1}{2} - \frac{\nu - 1}{2} \log_2 \frac{\nu - 1}{2}. \quad (29)$$

The asymptotic key rate is given by

$$R_{\text{asy}} = \beta I(x : y) - \chi(E : y) \quad (30)$$

$$= R(\beta, \mu, \eta, v_{\text{el}}, T, \xi). \quad (31)$$

Suppose that η and v_{el} are known and the parties have preliminary estimates of T and ξ . Then, for a target β , Alice can compute an optimal value μ_{opt} for the modulation μ by optimizing the asymptotic rate in Eq. (31).

C. Parameter estimation

In a realistic implementation of the protocol, the parties uses the quantum channel a finite number N of times. The first consequence of this finite-size scenario is that their knowledge of the channel parameters T and ξ is not perfect. Once the quantum communication is over, Alice and Bob declare m random instances $\{x_i\}$ and $\{y_i\}$ of their local variables x and y . From these values, they build the maximum-likelihood estimators $\hat{\tau}$ of the square-root transmissivity $\tau = \sqrt{T\eta}$ and $\hat{\sigma}_z^2$ of the noise σ_z^2 . These are given by

$$\hat{\tau} = \frac{\sum_{i=1}^m x_i y_i}{\sum_{i=1}^m x_i^2}, \quad (32)$$

$$\hat{\sigma}_z^2 = \frac{1}{m} \sum_{i=1}^m (y_i - \hat{\tau} x_i)^2. \quad (33)$$

For m sufficiently large, we have that, up to an error probability ϵ_{PE} , the channel parameters fall in the intervals

$$\tau \in [\hat{\tau} - \Delta_{\tau}, \hat{\tau} + \Delta_{\tau}], \quad (34)$$

$$\sigma_z^2 \in [\hat{\sigma}_z^2 - \Delta_{\sigma}, \hat{\sigma}_z^2 + \Delta_{\sigma}], \quad (35)$$

where

$$\Delta_{\tau} := w \sqrt{\frac{\hat{\sigma}_z^2}{m(\mu - 1)}}, \quad \Delta_{\sigma} := w \frac{\hat{\sigma}_z^2 \sqrt{2}}{\sqrt{m}}, \quad (36)$$

and w is expressed in terms of ϵ_{PE} via the inverse error function, i.e.,

$$w = \sqrt{2} \operatorname{erf}^{-1}(1 - \epsilon_{\text{PE}}). \quad (37)$$

Under the general model of detector described in Fig. 1, the parties have trusted levels of detector/setup efficiency η and electronic noise v_{el} . Knowing these values, they may derive the estimators for the transmissivity T and excess noise variance $\Xi := \eta T \xi$, i.e.,

$$\hat{T} = \frac{\hat{\tau}^2}{\eta}, \quad \hat{\Xi} = \hat{\sigma}_z^2 - 1 - v_{\text{el}}. \quad (38)$$

Then they may assume the “worst-case estimators”

$$T_m = \frac{(\hat{\tau} - \Delta_{\tau})^2}{\eta}, \quad \Xi_m = \hat{\Xi} + \Delta_{\sigma}, \quad (39)$$

so that $T \geq T_m$ and $\Xi \leq \Xi_m$ up to an error ϵ_{PE} .

In the next step, they compute an over-estimation of the Holevo bound in terms of T_m and Ξ_m , so that they may write the modified rate

$$R_m := \beta I(x : y) - \chi(E : y)|_{T_m, \Xi_m}. \quad (40)$$

Accounting for the number of signals sacrificed for PE, the actual rate in terms of bits per channel use is given by the rescaling

$$R_m \rightarrow \frac{n}{N} R_m, \quad (41)$$

where $n = N - m$ are the instances for key generation.

Note that, from the estimators \hat{T} and $\hat{\Xi}$, the parties may compute an estimator for the SNR, i.e.,

$$\widehat{\text{SNR}} = \frac{(\mu - 1)\eta \hat{T}}{1 + v_{\text{el}} + \hat{\Xi}}. \quad (42)$$

Therefore, in a practical implementation, the rate in Eq. (40) is replaced by the following expression

$$R_m = \beta I(x : y)|_{\hat{T}, \hat{\Xi}} - \chi(E : y)|_{T_m, \Xi_m}, \quad (43)$$

$$I(x : y)|_{\hat{T}, \hat{\Xi}} = \frac{1}{2} \log_2 \left(1 + \widehat{\text{SNR}} \right). \quad (44)$$

For fixed β , the parties could potentially optimize the SNR over the modulation parameter μ . In fact, before the quantum communication, they may use rough estimates about transmissivity and excess noise to compute value $\mu_{\text{opt}}(\beta)$ that maximizes the asymptotic key rate.

In a practical implementation, the data generated by the QKD protocol is sliced in $n_{\text{bks}} \gg 1$ blocks, each block being associated with the quantum communication of N points (modes). Assuming that the channel is sufficiently stable over time, the statistics (estimators and worst-case values) can be computed over

$$M := mn_{\text{bks}} \gg m \quad (45)$$

random instances, so that all the estimators (i.e., \hat{T} , $\hat{\Xi}$, $\widehat{\text{SNR}}$, T_m , and Ξ_m) are computed over M points and we replace $R_m \rightarrow R_M$ in Eq. (43), i.e., we consider

$$R_M = \beta I(x : y)|_{\hat{T}, \hat{\Xi}} - \chi(E : y)|_{T_M, \Xi_M}, \quad (46)$$

This also means that we consider an average of $m = M/n_{\text{bks}}$ points for PE in each block, and an average number of $n = N - M/n_{\text{bks}}$ key generation points from each block to be processed in the step of EC. Because N is typically large, the variations around the averages can be considered to be negligible, so that we may assume m and n to be the actual values for each block.

Finally note that, if the channel instead varies over a timescale comparable to the block size N (which is a condition that may occur in free-space quantum communications [12, 26]), then we may need to perform PE independently for each block. In this case, one would have a different rate for each block, so that the final key rate will be given by an average. However, for ground-based fiber-implementation, the channel is typically stable over long times, which is the condition assumed here.

D. Error correction

Once PE has been done, the parties process their remaining n pairs (key generation points) in a procedure of EC. Here we combine elements from various works [14, 17, 19, 27, 28]. The procedure can be broken down in steps of normalization, discretization, splitting, LDPC encoding/decoding, and EC verification.

1. Normalization

In each block of size N , Alice and Bob have n pairs $\{x_i, y_i\}$ of their variables x and y that are related by Eq. (3) and can be used for key generation. As a first step, Alice and Bob normalize their variables by dividing them by the respective standard deviations, i.e., [19]

$$x \rightarrow X := x/\sigma_x, \quad y \rightarrow Y := y/\sigma_y, \quad (47)$$

so that X and Y have the following CM

$$\Sigma_{XY} = \begin{pmatrix} 1 & \rho \\ \rho & 1 \end{pmatrix}. \quad (48)$$

Variables X and Y follow a standard normal bi-variate distribution with correlation $\rho = \mathbb{E}(XY)$, which is connected to the SNR by Eq. (14), where the latter is approximated by Eq. (42) in a practical scenario.

Under conditions of stability for the quantum communication channel, the normalization in Eq. (47) is performed over the entire record of nn_{bks} key generation points. Using the computed standard deviations σ_x and σ_y , we then build the strings $X^n = x^n/\sigma_x$ and $Y^n = y^n/\sigma_y$ for each block, starting from the corresponding n key generation points $x^n = \{x_i\}$ and $y^n = \{y_i\}$.

2. Discretization

Bob discretizes his normalized variable Y in a p -ary variable K with generic value $\kappa \in \{0, \dots, 2^p - 1\}$ being

an element of a Galois field $\mathcal{GF}(2^p)$. This is achieved as follows. As a first step, he sets a cut-off α such that $|Y| \leq \alpha$ occurs with negligible probability, which is approximately true for $\alpha \geq 3$. Then, Bob chooses the size $\delta = 2\alpha 2^{-p}$ of the intervals (bins) $[a_\kappa, b_\kappa]$ of his lattice, whose border points are given by [17]

$$a_\kappa = \begin{cases} -\infty & \text{for } \kappa = 0, \\ -\alpha + \kappa\delta & \text{for } \kappa > 0, \end{cases} \quad (49)$$

and

$$b_\kappa = \begin{cases} -\alpha + (\kappa + 1)\delta & \text{for } \kappa < 2^p - 1, \\ \infty & \text{for } \kappa = 2^p - 1. \end{cases} \quad (50)$$

Finally, for any value of $Y \in [a_\kappa, b_\kappa]$, Bob takes K equal to κ . Thus, for n points, the normalized string Y^n is transformed into a string of discrete values K^n . Note that this discretization technique is very basic. Indeed one could increase the performance by adopting bins of different sizes depending on the estimated SNR.

3. Splitting

Bob sets an integer value for q and computes $d = p - q$. Then, he splits his discretized variable in two parts $K = (\overline{K}, \underline{K})$, where the top variable \overline{K} is q -ary and the bottom variable \underline{K} is d -ary. Their values are defined by splitting the generic value κ in the following two parts

$$\overline{\kappa} = \frac{\kappa - (\kappa \bmod 2^d)}{2^d}, \quad \underline{\kappa} = (\kappa \bmod 2^d). \quad (51)$$

In other words, we have

$$\kappa = \overline{\kappa}2^d + \underline{\kappa}. \quad (52)$$

With the top variable \overline{K} , Bob creates 2^q *super-bins* with each super-bin containing 2^d bins associated with the bottom variable \underline{K} . See also Fig. 2.

Repeating this for n points provides a string of values \overline{K}^n for the super-bins and another string for the relative bin-positions \underline{K}^n . The most significant string \overline{K}^n is locally processed via an LDPC code (more details below), while the least-significant string \underline{K}^n is side-information that is revealed through the public channel.

4. LDPC encoding and decoding

Bob constructs an $l \times n$ parity check matrix \mathbf{H} with q -ary entries from $\mathcal{GF}(2^q)$ according to Ref. [27]. This matrix is applied to the top string \overline{K}^n to derive the l -long syndrome $K_{\text{sd}}^l = \mathbf{H}\overline{K}^n$, where the matrix-vector product is defined in $\mathcal{GF}(2^q)$. The syndrome is sent to

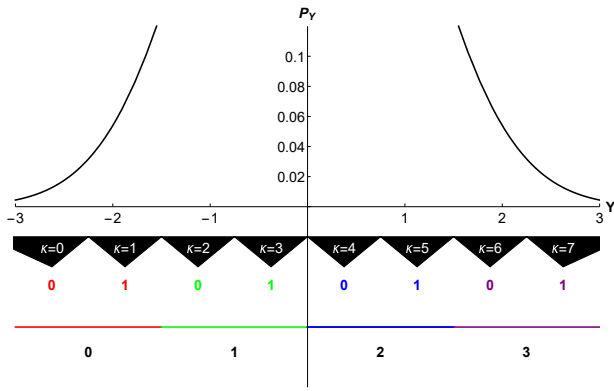


FIG. 2: Discretization and splitting with $\alpha = 3$, $p = 3$ and $q = 2$. The variable Y follows a normal distribution P_Y so that the probability of $|Y| > 3$ is assumed to be negligible. Variable Y and the bins defined in Eqs. (49) and (50) identify a discrete variable K with values $\kappa = 0, \dots, 7$ (black triangles). During the splitting stage, each bin can be described by two numbers: $\bar{\kappa} = 0, \dots, 3$ associated with $q = 2$, and $\underline{\kappa} = 0, 1$ associated with $d = p - q = 1$. We see that 2^d bins belong to each *super-bin* $\bar{\kappa}$ (coloured intervals). Bob uses the parity check matrix of a non-binary LDPC code to encode the information $\bar{\kappa}$ related to the *super-bin* while the position $\underline{\kappa}$ of the bin inside the super-bin is broadcast through the public channel.

Alice together with the direct communication of the bottom string \underline{K}^n . The parity check matrix is associated with an LDPC code [14], which may encode $k = n - l$ source symbols into n output symbols, so that it has rate

$$R_{\text{code}} := k/n = 1 - R_{\text{syn}}, \quad R_{\text{syn}} := l/n. \quad (53)$$

What value of R_{code} to use and, therefore, what matrix \mathbf{H} to build is explained afterwards in this subsection.

From the knowledge of syndrome K_{sd}^l , Bob's bottom string \underline{K}^n and her local string X^n , Alice decodes Bob's top string \bar{K}^n . This is done via an iterative belief propagation algorithm [14] where, in every iteration, she updates a codeword likelihood function. The initial likelihood function before any iteration comes from the *a priori* probabilities

$$P(\bar{K}|X, \underline{K}) = \frac{P(\bar{K}, \underline{K}|X)}{\sum_{\bar{K}} P(\bar{K}, \underline{K}|X)} \quad (54)$$

where

$$P(\bar{K}, \underline{K}|X) = P(K|X) \quad (55)$$

$$= \frac{1}{2} \text{erf} \left(\frac{b_{\kappa} - \rho x / \sigma_x}{\sqrt{2(1 - \rho^2)}} \right) - \frac{1}{2} \text{erf} \left(\frac{a_{\kappa} - \rho x / \sigma_x}{\sqrt{2(1 - \rho^2)}} \right). \quad (56)$$

At any iteration $\leq \text{iter}_{\text{max}}$ Alice finds the argument that maximizes the likelihood function. If the syndrome of this argument is equal to K_{sd}^l , then the argument forms her guess \hat{K}^n of Bob's top string \bar{K}^n . However, if this syndrome matching test (SMT) is not satisfied within the

maximum number of iterations iter_{max} then the block is discarded. The possibility of failure in the SMT reduces the total number of input blocks from n_{bks} to $n_{\text{SMT}} = p_{\text{SMT}} n_{\text{bks}}$ where p_{SMT} is the probability of successful matching within the established iter_{max} iterations.

Let us compute the LDPC rate R_{code} to be used. First notice how Alice and Bob's mutual information decreases as a consequence of the classical data processing inequality [23] applied to the procedure. We have

$$I(x : y) \geq I(X : Y) \quad (57)$$

$$\geq I(X : K) = H(K) - H(K|X) \quad (58)$$

$$\geq H(K) - \text{leak}_{\text{EC}} \quad (59)$$

where $\text{leak}_{\text{EC}} \geq H(K|X)$ comes from the Wolf-Slepian limit [24, 25] and $H(K)$ is the Shannon entropy of K , which can be computed over the entire record of nn_{bks} key generation points (under stability conditions). In particular, we may write the approximation [23, Ch. 8]

$$H(K) \simeq h(Y) - \log_2 \delta = \frac{1}{2} \log_2 2\pi e - \log_2 \delta \quad (60)$$

$$= p + \log_2 [\sqrt{\pi e / 2} \alpha^{-1}]. \quad (61)$$

where we have also used $\sigma_Y = 1$ and $\delta = 2\alpha/2^p$.

In Eq. (59) the leakage leak_{EC} is upper-bounded by the equivalent number of bits per use that are broadcast after the LDPC encoding in each block, i.e.,

$$\text{leak}_{\text{EC}} \leq d + R_{\text{syn}} q. \quad (62)$$

Therefore, we may write

$$I(x : y) \geq \beta I(x : y) := H(K) + R_{\text{code}} q - p. \quad (63)$$

Note that, in a practical implementation, Alice and Bob do not access $I(x : y)$ but rather $I(x : y)|_{\hat{T}, \hat{\Xi}}$ from Eq. (44). Therefore, considering this modification in Eq. (63), we more precisely derive

$$\beta I(x : y)|_{\hat{T}, \hat{\Xi}} = H(K) + R_{\text{code}} q - p, \quad (64)$$

so that the rate in Eq. (46) becomes

$$R_M^{\text{EC}} = H(K) + R_{\text{code}} q - p - \chi(E : y)|_{T_M, \Xi_M} \quad (65)$$

$$\simeq R_{\text{code}} q + \log_2 [\sqrt{\pi e / 2} \alpha^{-1}] - \chi(E : y)|_{T_M, \Xi_M}. \quad (66)$$

From Eqs. (44) and (64), we see that the LDPC code must be chosen to have rate

$$R_{\text{code}} = q^{-1} \left[\frac{\beta}{2} \log_2 \left(1 + \widehat{\text{SNR}} \right) + p - H(K) \right] \quad (67)$$

$$\simeq q^{-1} \log_2 \alpha \sqrt{\frac{2(1 + \widehat{\text{SNR}})^{\beta}}{\pi e}}, \quad (68)$$

for some estimated SNR. A value of the reconciliation efficiency β is acceptable only if we can choose parameters $\alpha \geq 3$ and q [29] such that $R_{\text{code}} \leq 1$. Once R_{code} is known, the sparse parity check matrix \mathbf{H} of the LDPC code can be constructed following Ref. [27].

5. Verification

An important final step in the EC procedure is the verification of the n_{SMT} error-corrected blocks that have successfully passed the SMT. For each of these blocks, the parties possess two n -long q -ary strings with identical syndromes, i.e., Bob's top string \overline{K}^n and Alice's guess \widehat{K}^n . The parties convert their strings into a binary representation, $\overline{K}_{\text{bin}}^n$ and $\widehat{K}_{\text{bin}}^n$, so that each of them is qn bit long. In the next step, Alice and Bob compute t -bit long hashes of their converted binary strings following Ref. [28] (universal hash functions are used because of their resistance to collisions). In particular, they set $t = \lceil -\log_2 \epsilon_{\text{cor}} \rceil$, where ϵ_{cor} is known as 'correctness'.

Then, Bob discloses his hash to Alice, who compares it with hers. If the hashes are identical, the verification stage is deemed successful. The two strings $\overline{K}_{\text{bin}}^n$ and $\widehat{K}_{\text{bin}}^n$ are identical up to a small error probability $2^{-t} \leq \epsilon_{\text{cor}}$. In such a case, the associated bottom string \underline{K}^n held by both parties is converted by both parties into binary $\underline{K}_{\text{bin}}^n$ and appended to the respective strings, i.e., $\overline{K}_{\text{bin}}^n \rightarrow \overline{K}_{\text{bin}}^n \underline{K}_{\text{bin}}^n$ and $\widehat{K}_{\text{bin}}^n \rightarrow \widehat{K}_{\text{bin}}^n \underline{K}_{\text{bin}}^n$. Such binary concatenations are promoted to the next step of PA.

By contrast, if the hashes are different, then the two post-processed strings are discarded (together with the public bottom string). We therefore have a probability of success associated with the hash verification test, that we denote by p_{ver} . This is implicitly connected with ϵ_{cor} . In fact, if we decrease ϵ_{cor} we increase the length of the hashes to verify, and we therefore increase the probability of spotting an uncorrected error in the strings, which leads to a reduction of the success probability p_{ver} .

Thus, combining the possible failures in the syndrome and hash tests, we have a total probability of success for EC, which is given by

$$p_{\text{EC}} = p_{\text{SMT}} p_{\text{ver}} := 1 - p_{\text{FER}}, \quad (69)$$

where p_{FER} is known as 'frame error rate' (FER).

Note that the effective value of p_{EC} depends not only on ϵ_{cor} but also on the specific choice for the LDPC code. In particular, in the presence of a very noisy channel, using a high-rate LDPC code (equivalent to a high value of β) implies low correction performances and, therefore, a low value for p_{EC} (SMT and/or hash test tend to fail). By contrast, the use of a low-rate EC code (low value of β) implies a high value for p_{EC} (good performance for both SMT and hash test). Thus, there is an implicit trade-off between p_{EC} and β . For fixed values of ϵ_{cor} and β , the value of p_{EC} (success of the EC test) still depends on the channel noise, so that it needs to be carefully calculated from the experimental/simulation points.

E. Privacy amplification and composable-secure finite-size key

The final step is that of PA, after which the secret key is generated. Starting from the original n_{bks} blocks (each being N -size), the parties derive $p_{\text{EC}} n_{\text{bks}}$ successfully error-corrected binary strings

$$S := \overline{K}_{\text{bin}}^n \underline{K}_{\text{bin}}^n \simeq \widehat{S} := \widehat{K}_{\text{bin}}^n \underline{K}_{\text{bin}}^n, \quad (70)$$

each string containing np bits. In this final step, all the surviving error-corrected strings are compressed into shorter strings that are decoupled from Eve (up to a small error probability that we discuss below). This compression step can be implemented on each sequence individually, or globally on a concatenation of sequences, which is the approach adopted here and certainly valid under conditions of channel stability.

Concatenating their local $p_{\text{EC}} n_{\text{bks}}$ error-corrected strings, Alice and Bob construct two long binary sequences $\mathbf{S} \simeq \widehat{\mathbf{S}}$, each having $\tilde{n} := p_{\text{EC}} n_{\text{bks}} np$ bits. Each of these sequences will be compressed to a final secret key of $r := p_{\text{EC}} n_{\text{bks}} \tilde{n} \tilde{R}$ bits, where \tilde{R} is determined by the composable key rate (see below). The compression is achieved via universal hashing by applying a Toeplitz matrix $\mathbf{T}_{r, \tilde{n}}$. Thus, from their sequences, Alice and Bob finally retrieve the secret key

$$\mathbf{K} = \mathbf{T}_{r, \tilde{n}} \mathbf{S} \simeq \mathbf{T}_{r, \tilde{n}} \widehat{\mathbf{S}}. \quad (71)$$

An important parameter to consider for the step of PA is the 'secrecy' ϵ_{sec} , which bounds the distance between the final key and an ideal key from which Eve is completely decoupled. Technically, one further decomposes $\epsilon_{\text{sec}} = \epsilon_s + \epsilon_h$, where ϵ_s is a smoothing parameter ϵ_s and ϵ_h is a hashing parameter. These PA epsilon parameters are combined with the other ones from the steps of PE and EC to form the overall ϵ -security of the protocol

$$\epsilon = p_{\text{EC}} \epsilon_{\text{PE}} + \epsilon_{\text{cor}} + \epsilon_{\text{sec}}. \quad (72)$$

A typical choice is to set $\epsilon_s = \epsilon_h = \epsilon_{\text{cor}} = \epsilon_{\text{PE}} = 2^{-32} \simeq 2.3 \times 10^{-10}$, so that $\epsilon \lesssim 10^{-9}$ for any p_{EC} .

For success probability p_{EC} and ϵ -security against collective (Gaussian) attacks, the secret key rate of the protocol (in terms of bits per channel use) takes the form [12]

$$R = \frac{np_{\text{EC}}}{N} \tilde{R}, \quad \tilde{R} := \left(R_M^{\text{EC}} - \frac{\Delta_{\text{AEP}}}{\sqrt{n}} + \frac{\Theta}{n} \right), \quad (73)$$

where R_M^{EC} is given in Eq. (65) and the extra terms are

$$\Delta_{\text{AEP}} := 4 \log_2 \left(2^{1+p/2} + 1 \right) \sqrt{\log_2 \left(\frac{18}{p_{\text{EC}}^2 \epsilon_s^4} \right)}, \quad (74)$$

$$\Theta := \log_2 [p_{\text{EC}} (1 - \epsilon_s^2/3)] + 2 \log_2 \sqrt{2} \epsilon_h. \quad (75)$$

Note that the discretization bits p appear in Δ_{AEP} .

The practical secret key rate in Eq. (73) can be compared with a corresponding theoretical rate

$$R_{\text{theo}} = \frac{n\tilde{p}_{\text{EC}}}{N} \left(R_M^* - \frac{\tilde{\Delta}_{\text{AEP}}}{\sqrt{n}} + \frac{\tilde{\Theta}}{n} \right), \quad (76)$$

where \tilde{p}_{EC} is guessed, with $\tilde{\Delta}_{\text{AEP}}$ and $\tilde{\Theta}$ being computed on that guess. Then, we have

$$R_M^* = \tilde{\beta} I(x : y)|_{T, \Xi} - \chi(E : y)|_{T_M^*, \Xi_M^*}, \quad (77)$$

where $\tilde{\beta}$ is also guessed, and the various estimators are approximated by their mean values, so that $\hat{T} \simeq T$, $\hat{\Xi} \simeq \Xi = \eta T \xi$ and we have set

$$T_M^* = \left(\sqrt{T} - w \sqrt{\frac{\sigma_z^2}{M\eta(\mu-1)}} \right)^2, \quad (78)$$

$$\Xi_M^* = \Xi + w\sigma_z^2 \sqrt{\frac{2}{M}}, \quad (79)$$

with w depending on ϵ_{PE} as in Eq. (37).

III. PROTOCOL SIMULATION AND DATA PROCESSING

Here we sequentially go over the steps of the protocol and its post-processing, as they need to be implemented in a numerical simulation or an actual experimental demonstration. We provide more technical details and finally present the pseudocode of the entire procedure.

A. Main parameters

We start by discussing the main parameters related to the physical setup, communication channel and protocol. Some of these parameters are taken as input, while others need to be estimated by the parties, so that they represent output values of the simulation.

Setup: Main parameters are Alice's modulation variance μ , Bob's trusted levels of local efficiency η , and electronic noise v_{el} . These are all input values.

Channel: Main parameters are the effective transmissivity T , and excess noise ξ . These are input values to our simulation, which are used to create the input-output relation of Eq. (3). In an experimental implementation, these values are generally unknown and Eq. (3) comes from the experimental data.

Protocol: Main parameters are the number of blocks n_{bks} , the size of each block N , the total number M of instances for PE, the various epsilon parameters $\epsilon_{\text{s,h},\dots}$ and the p -bit discretization, so that the alphabet size is $D = 2^p$. These are all input values. Output values are the estimators \hat{T} , $\hat{\Xi}$, T_M , Ξ_M , the EC probability of success p_{EC} , the reconciliation parameter β and the final rate R .

In Tables I and II, we summarize the main input and output parameters. In Table III, we schematically show the formulas for other related parameters.

parameter	description
L	Channel length (km)
A	Attenuation rate (dB/km)
ξ	Excess noise
η	Detector/Setup efficiency
v_{el}	Electronic noise
β	Reconciliation parameter
n_{bks}	Number of blocks
N	Block size
M	Number of PE runs
p	Discretization bits
q	Most significant (top) bits
α	Phase-space cut-off
iter_{max}	Max number of EC iterations
$\epsilon_{\text{PE, s, h, corr}}$	Epsilon parameters
μ	Modulation variance

TABLE I: Main input parameters

parameter	description
μ_{opt}	Optimal modulation variance
R_{asy}	Asymptotic key rate
$\hat{T}, \hat{\Xi}, T_M, \Xi_M$	Estimators
$\widehat{\text{SNR}}$	Estimated SNR
R_{code}	Code rate
p_{EC}	EC success probability
fnd_{rnd}	EC syndrome matching round
r	Final key length
R	Composable key rate
\mathbf{K}	Final key
ε	ε -security

TABLE II: Main output parameters

B. Quantum communication

The process of quantum communication can be simplified in the following two steps before and after the action of the channel.

Preparation: Alice encodes Nn_{bks} instances $\{x_i\}$ of the mean x of the generic quadrature \hat{x} , such that $x \sim \mathcal{N}(0, \mu - 1)$. In the experimental practice, the two conjugate quadratures are independently encoded in the amplitude of a coherent state, but only one of them will survive after the procedure of sifting (here implicitly assumed).

parameter	description	formula
T	Channel transmissivity	$10^{-AL/10}$
σ_z^2	Noise variance	$1 + v_{\text{el}} + \eta T \xi$
Ξ	Excess noise variance	$\eta T \xi$
ω	Thermal noise	$\frac{T \xi - T + 1}{1 - T}$
\mathcal{X}	Equivalent noise	$\xi + \frac{1 + v_{\text{el}}}{T \eta}$
SNR	Signal-to-noise ratio	$\frac{\mu - 1}{\chi}$
m	PE instances per block	M/n_{bks}
n	Key generation points per block	$N - m$
FER	Frame error rate	$1 - p_{\text{EC}}$
GF	Number of the \mathcal{GF} elements	2^q
δ	Lattice step in phase space	$\frac{\alpha}{2^{p-1}}$
d	Least significant (bottom) bits	$p - q$
t	Verification hash output length	$\lceil -\log_2 \epsilon_{\text{cor}} \rceil$
ρ	Correlation coefficient	$\sqrt{\frac{\text{SNR}}{1 + \text{SNR}}}$
\tilde{n}	Total bit string length after EC	$n p n_{\text{bks}} p_{\text{EC}}$

TABLE III: Related parameters

Measurement: After the channel and the projection of (a randomly-switched) homodyne detection, Bob decodes Nn_{bks} instances $\{y_i\}$ of $y = \sqrt{T}\eta x + z$, where the noise variable $z \sim \mathcal{N}(0, \sigma_z^2)$ has variance σ_z as in Eq. (4).

As mentioned above, it is implicitly assumed that Alice and Bob perform a sifting stage where Bob classically communicates to Alice which quadrature he has measured (so that the other quadrature is discarded).

C. Parameter estimation

The stage of PE is described by the following steps.

Random positions: Alice randomly picks M positions $i \in [1, Nn_{\text{bks}}]$, say $\{i_u\}_{u=1}^M$. On average $m = M/n_{\text{bks}}$ positions are therefore picked from each block, and $n = N - m$ points are left for key generation in each block (for large enough blocks, the spread around these averages is negligible).

Public declaration: Using a classical channel, Alice communicates the M pairs $\{i_u, x_{i_u}\}_{u=1}^M$ to Bob.

Estimators: Bob sets a PE error ϵ_{PE} . From the pairs $\{x_{i_u}, y_{i_u}\}_{u=1}^M$, he then computes the estimators \hat{T} and $\hat{\Xi}$, and the worst-case estimators T_M and Ξ_M (see formulas in Sec. II C).

Early termination: Bob checks the threshold condition $I(x : y)|_{\hat{T}, \hat{\Xi}} > \chi(E : y)|_{T_M, \Xi_M}$, which is computed in terms of the estimators \hat{T} and $\hat{\Xi}$, and worst-case estimators T_M and Ξ_M (associated with ϵ_{PE}). If the threshold condition is not satisfied, then the protocol is aborted.

D. Error correction

The procedure of EC is performed on each block of size N and consists of the following steps.

Normalization: For key generation, Alice and Bob have n pairs $\{x_i, y_i\}$ of their variables x and y that are related by Eq. (3). As a first step, Alice and Bob normalize their variables x and y according to Eq. (47), therefore creating X and Y .

Discretization: Bob sets the cut-off value α and the step $\delta = \alpha 2^{1-p}$ of his lattice, whose generic bin $Y[a_\kappa, b_\kappa]$ is defined by Eqs. (49) and (50). Then, he discretizes his normalized variable Y into a p -ary variable K with generic value $\kappa \in \{0, \dots, 2^p - 1\}$ with the following rule: For any value of his variable $Y \in [a_\kappa, b_\kappa]$, Bob takes K equal to κ .

Splitting: Bob sets an integer value for q and computes $d = p - q$. From his discretized variable K , he creates the top q -ary variable \bar{K} and the bottom d -ary variable \underline{K} , whose generic values $\bar{\kappa}$ and $\underline{\kappa}$ are defined by Eq. (51). For n points, he therefore creates a string \bar{K}^n which is locally processed via an LDPC code (see below), and another string \underline{K}^n which is revealed through the public channel.

LDPC encoding: From the estimator $\widehat{\text{SNR}}$, the entropy $H(K)$, and a target reconciliation efficiency β , the parties use Eq. (67) to derive the rate R_{code} of the LDPC code. They then build its $l \times n$ parity-check matrix \mathbf{H} with q -ary entries from $\mathcal{GF}(2^q)$, using the procedure of Ref. [27], i.e., (i) the column weight d_v (number of nonzero elements in a column) is constant and we set $d_v = 2$; (ii) the row weight d_c adapts to the formula $R_{\text{code}} = 1 - d_v/d_c$ and is as uniform as possible; and (iii) the overlap (inner product between two columns) is never larger than 1.

Once \mathbf{H} is constructed, Bob computes the syndrome $K_{\text{sd}}^l = \mathbf{H} \bar{K}^n$, which is sent to Alice together with the bottom string \underline{K}^n .

LDPC decoding: From the knowledge of the syndrome K_{sd}^l , Bob's bottom string \underline{K}^n and her local string X^n , Alice decodes her guess \hat{K}^n of Bob's top string \bar{K}^n . This is done via a sum-product algorithm [14], where in each iteration $\text{iter} < \text{iter}_{\text{max}}$ Alice updates a suitable likelihood function with initial value given by the *a-priori* probabilities in Eq. (56). If the syndrome of \hat{K}^n is equal to K_{sd}^l , then Alice's guess \hat{K}^n of Bob's top string \bar{K}^n is promoted to the next verification step. If the syndrome matching test fails for iter_{max} iterations, the block is discarded and one registers the frequency/probability $1 - p_{\text{SMT}}$ of this event. For more details of the sum-product algorithm see Appendix B.

Verification: Each pair of promoted strings \bar{K}^n and \hat{K}^n is converted to binary \bar{K}_{bin}^n and \hat{K}_{bin}^n . Over these, the parties compute hashes of $t = \lceil -\log_2 \epsilon_{\text{cor}} \rceil$ bits. Bob discloses his hash to Alice, who compares it with hers. If the hashes are identical, the parties convert the corresponding bottom string \underline{K}^n into binary $\underline{K}_{\text{bin}}^n$ and promote the two concatenations

$$S := \bar{K}_{\text{bin}}^n \underline{K}_{\text{bin}}^n \simeq \hat{S} := \hat{K}_{\text{bin}}^n \underline{K}_{\text{bin}}^n \quad (80)$$

to the next step of PA. By contrast, if the hashes are different, then \bar{K}_{bin}^n and \hat{K}_{bin}^n are discarded, together with \underline{K}^n . The parties compute the frequency/probability of success of the hash verification test p_{ver} and derive the overall success probability of EC $p_{\text{EC}} = p_{\text{SMTPver}} = 1 - p_{\text{FER}}$.

In more detail, the strings \bar{K}_{bin}^n and \hat{K}_{bin}^n are broken into Q -bit strings that are converted to Q -ary numbers forming the strings $\bar{K}_Q^{n'}$ and $\hat{K}_Q^{n'}$ with $n' = nq/Q$ symbols for $Q > q$. In case nq/Q is not an integer, the strings \bar{K}_{bin}^n and \hat{K}_{bin}^n are padded with sq zeros so that $n' = (n+s)q/Q \in \mathbb{N}$. Bob then derives independent uniform random integers $v_i = 1, \dots, 2^{Q^*} - 1$, where v_i is odd, and an integer $u = 0, \dots, 2^{Q^*} - 1$, for $i = 1, \dots, n'$ and $Q^* \leq Q + t - 1$ with $\epsilon_{\text{cor}} \leq 2^{-t}$ being the target collision probability. After Bob communicates his choice of universal families to Alice, they both hash each of the Q -ary numbers and combine the results according to the following formula [28]

$$\tilde{h}(\mathbf{x}) = \left(\sum_{i=1}^{n'} v_i x_i \right) + u, \quad (81)$$

where $\mathbf{x} = \bar{K}_Q^{n'}$ (for Bob) or $\hat{K}_Q^{n'}$ (for Alice). Summation and multiplication in Eq. (81) are modulo 2^{Q^*} . In practice, this is done by discarding the overflow (number of bits over Q^*) of $\tilde{h}(\mathbf{x})$. Then they keep only the first t bits to form the hashes (where typically $t = 32$).

E. Privacy amplification

After EC, Alice and Bob are left with $p_{\text{EC}} n_{\text{bks}}$ successfully error-corrected binary strings, each of them being represented by Eq. (80) and containing np bits. By concatenation, they build two long binary sequences $\mathbf{S} \simeq \hat{\mathbf{S}}$, each having $\tilde{n} := p_{\text{EC}} n_{\text{bks}} np$ bits. For the chosen level of secrecy ε_{sec} , the parties compute the overall epsilon security ε from Eq. (72) and the key rate $R = \frac{n_{\text{PEC}}}{N} \tilde{R}$ according to Eq. (73). Finally, the sequences $\mathbf{S} \simeq \hat{\mathbf{S}}$ are compressed into a final secret key of length $r := p_{\text{EC}} n_{\text{bks}} n \tilde{R}$ bits, by applying a Toeplitz matrix $\mathbf{T}_{r, \tilde{n}}$ so that the secret key is given by Eq. (71).

F. Pseudocode of the procedure

In Algorithm 1, we present the entire pseudocode of the procedure, whose steps have been implemented in our Python library CVQKDsim [11].

Algorithm 1 High-Level Routine Overview

```

1:  $L, A, \eta, \xi, v_{\text{el}}, n_{\text{bks}}, N, M, \epsilon_{\text{PE}}, \epsilon_s, \epsilon_h, \epsilon_{\text{cor}}, \beta, \text{iter}_{\text{max}}, p, q, \alpha \leftarrow$ 
   Input_Values_Definition()
2:  $T, \sigma_z^2, \Xi, m, n, t, \text{GF}, \delta, d \leftarrow \text{Dependent_Values}()$ 
3: Validity_Checks()
4: if is_mu_optimal then
5:    $\mu_{\text{opt}} \leftarrow \text{Optimal_Modulation}()$ 
6: else
7:    $\mu \leftarrow \text{user_input}$ 
8: end if
9: for blk = 1, 2, ..., n_{\text{bks}} do
10:   $x[\text{blk}] \leftarrow \text{State_Preparation}()$ 
11:   $y[\text{blk}] \leftarrow \text{State_Transmission}()$ 
12:   $y[\text{blk}] \leftarrow \text{State_Measurement}()$ 
13:   $x[\text{blk}] \leftarrow \text{Key_Sifting}()$ 
14: end for
15:  $R_{\text{asy}}, I(x : y)|_{T, \Xi}, \chi(E : y)|_{T, \Xi} \leftarrow \text{Rate_Calculation}()$ 
16:  $\{i_u, x_{i_u}\}_{u=1}^M, \{i_u, y_{i_u}\}_{u=1}^M \leftarrow \text{Sacrificed_States_Selection}()$ 
17:  $\hat{T}, \hat{\Xi}, T_M, \Xi_M \leftarrow \text{Parameter_Estimation}()$ 
18:  $R_M, I(x : y)|_{\hat{T}, \hat{\Xi}}, \chi(E : y)|_{T_M, \Xi_M} \leftarrow \text{Rate_Calculation}()$ 
19: if  $I(x : y)|_{\hat{T}, \hat{\Xi}} \leq \chi(E : y)|_{T_M, \Xi_M}$  then
20:   Abort_Protocol()
21: end if
22:  $X, Y \leftarrow \text{Normalization}()$ 
23:  $\widehat{\text{SNR}}, \rho \leftarrow \text{Code_Estimations}()$ 
24: for blk = 1, 2, ..., n_{\text{bks}} do
25:    $K[\text{blk}] \leftarrow \text{Discretization}()$ 
26:    $\bar{K}[\text{blk}], \underline{K}[\text{blk}] \leftarrow \text{Splitting}()$ 
27:    $p_{\bar{K}|X, \underline{K}}[\text{blk}] \leftarrow \text{A_Priori_Probabilities_Calculation}()$ 
28: end for
29:  $R_{\text{code}}, H(K) \leftarrow \text{Code_Rate_Calculation}()$ 
30:  $\mathbf{H} \leftarrow \text{LDPC_Code_Generation}()$ 
31: for blk = 1, 2, ..., n_{\text{bks}} do
32:    $\bar{K}_{\text{sd}}^l[\text{blk}] \leftarrow \text{Bob_Syndrome_Calculation}()$ 
33:    $\hat{K}^n[\text{blk}], \text{fnd}, \text{rnd}_{\text{fnd}} \leftarrow \text{Non_Binary_Decoding}()$ 
34:    $\hat{K}_{\text{bin}}^n[\text{blk}], \bar{K}_{\text{bin}}^n[\text{blk}], \underline{K}_{\text{bin}}^n[\text{blk}] \leftarrow \text{Bin_Conversion}()$ 
35:    $\text{hash}_\text{verified}[\text{blk}] \leftarrow \text{Verification}()$ 
36:   if is_hash_verified[\text{blk}] then
37:      $\hat{S}[\text{blk}] \leftarrow \text{Concatenate}(\hat{K}_{\text{bin}}^n[\text{blk}], \underline{K}_{\text{bin}}^n[\text{blk}])$ 
38:      $S[\text{blk}] \leftarrow \text{Concatenate}(\bar{K}_{\text{bin}}^n[\text{blk}], \underline{K}_{\text{bin}}^n[\text{blk}])$ 
39:   end if
40: end for
41:  $p_{\text{EC}}, \text{FER} \leftarrow \text{Frame_Error_Rate_Calculation}()$ 
42:  $R, r, \tilde{n}, \varepsilon \leftarrow \text{Composable_Rate_Calculation}()$ 
43: if  $R > 0$  then
44:   for blk = 1, 2, ..., p_{\text{EC}} n_{\text{bks}} do
45:      $\hat{\mathbf{S}} \leftarrow \text{Append}(\hat{S}[\text{blk}])$ 
46:      $\mathbf{S} \leftarrow \text{Append}(S[\text{blk}])$ 
47:   end for
48:    $\mathbf{K} \leftarrow \text{Privacy_Amplification}()$ 
49: end if
50: Information_Logging()

```

IV. SIMULATION RESULTS

We are particularly interested in short-range high-rate implementations of CV-QKD, over distances of around 5 km in standard optical fiber. Even in this regime of relatively-high SNR, to get a positive value for the composable secret key rate, we need to consider a block size N of the order of at least 10^5 . The choice of the reconciliation efficiency β is also important, as a positive rate cannot be achieved when the value of β is too low. Sample parameters, for which one achieves a positive R are given in Table IV. In this choice of parameters, Alice's modulation variance μ is chosen so that $\text{SNR} = 12$. As we can see from Fig. 3, positive values for the composable secret-key rate are indeed achievable for block sizes with $N > 10^5$ and, as expected, the key rate grows as the block size increases, while all of the simulations attained $p_{\text{EC}} \geq 0.98$. The numerical values of the rate are good, since a key rate of 10^{-1} bits/use corresponds to 500 kbits/sec with a relatively-slow clock of 5 MHz.

In Fig. 4, we also show the behavior of the composable secret key rate versus distance L expressed in km of standard optical fiber. We adopt the input parameters specified in Table IV and we use blocks of size $N = 1.5 \times 10^5$ and $N = 2 \times 10^5$, with reconciliation efficiency β taking values greater than 92%. As we can see from the figure, high rates can be achieved at short distances, of the order of 0.5 bits/use at $L = 1$ km, and down to about 0.01 bits/use at $L = 6$ km.

In Fig. 5, we analyze the robustness of the protocol with respect to the amount of untrusted excess noise in the quantum communication channel (even though this parameter may also include any other imperfection coming from the experimental setup). As we can see from the figure, positive key rates are achievable up to relative-high values of ξ up to 0.07.

Figs. 6, 7 and 8 explore different quantities of interest (FER, rate, and EC rounds) as a function of the SNR and for various choices of the number p of discretization bits. The parameters used in the simulations are given in Table IV, where μ is variable and adapted to attain the desired SNR. The choices for the reconciliation efficiency β (shown in the right side of the table) are made according to the following rationale: (i) because a regular LDPC code only achieves a specific value of R_{code} , β is chosen so that R_{code} from Eq. (67) matches R_{code} of a regular LDPC code with high numerical accuracy; (ii) β is high enough so that a positive key rate can be achieved for various values of p for the same SNR; and (iii) β is low enough so that only a few EC rounds exceed the iteration limit iter_{max} (if β is too high, this limit is exceeded and FER increases).

Fig. 6 shows the FER for different values of SNR. As seen, the FER is higher for lower SNR and drops as the SNR increases. However, this drop happens only when the chosen β is appropriately low for its respective SNR. For the case of $\text{SNR} = 11$, choosing $\beta = 0.932$ leads to a spike in the FER with respect to the other choice

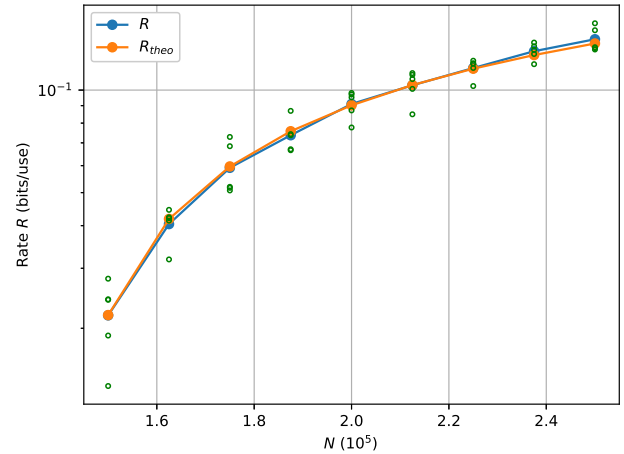


FIG. 3: Composable secret key rate R (bits/use) versus the block size N for $\text{SNR} = 12$. We compare the rate of Eq. (73) from the simulations (green points) and its average (blue line) with the theoretical rate of Eq. (76) (orange line), where the theoretical guesses for $\tilde{\beta}$ and \tilde{p}_{EC} are chosen compatibly with the simulations. In particular, we set $\tilde{\beta} = \beta = 0.9225$. Then, because all simulations provided $p_{\text{EC}} \geq 0.98$, we set $\tilde{p}_{\text{EC}} = 0.99$. The step of N is 12500. See Table IV for the list of input parameters used in the simulations.

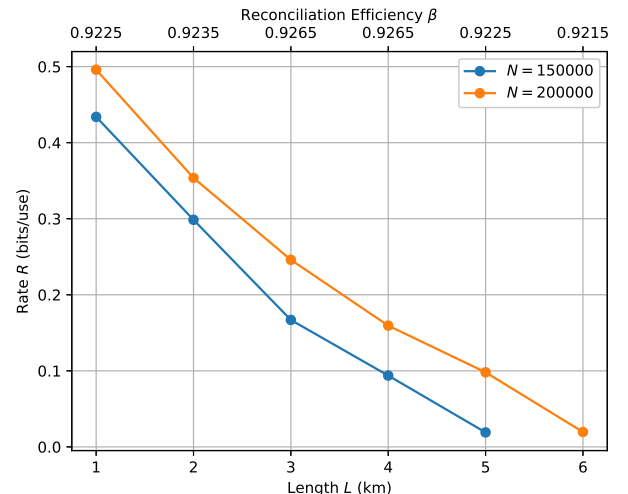


FIG. 4: Composable secret key rate R (bits/use) versus the channel length L (km). Here we use $N = 1.5 \times 10^5$ (blue line) and $N = 2 \times 10^5$ (orange line). The values of the reconciliation efficiency β are shown on the top axis. Other parameters are taken as in Table IV.

$\beta = 0.9075$. This happens because, for the higher value of β , significantly more rounds are needed to decode the frames (as seen in Fig. 8). Having set a maximum iteration limit $\text{iter}_{\text{max}} = 100$, it is not possible for some frames to be decoded. An increase in the reconciliation efficiency requires a corresponding increase in the maximum number of iterations. Said in other terms, higher values of β can only be achieved by paying the price of a slower decoding process. However, despite the discarded frames, the higher value of β still manages to yield a bet-

Parameter	Value (Fig. 3)	Value (Fig. 4)	Value (Fig. 5)	Value (Figs. 6-8)	SNR	β	R_{code}	d_c
L	5	variable	3	5	6	0.89	0.75	8
A	0.2	0.2	0.2	0.2	7	0.905	0.777	9
ξ	0.01	0.01	variable	0.01	8	0.912	0.8	10
η	0.8	0.8	0.8	0.8	9	0.912	0.818	11
v_{el}	0.1	0.1	0.05	0.1	10	0.91	0.833	12
β	0.9225	variable	variable	variable	11 _a	0.9075	0.846	13
n_{bks}	100	100	100	100	11 _b	0.932	0.857	14
N	$1.5 - 2.5 \times 10^5$	$(1.5, 2) \times 10^5$	2×10^5	2×10^5	12	0.9225	0.866	15
M	$0.1n_{\text{bks}}N$	$0.1n_{\text{bks}}N$	$0.1n_{\text{bks}}N$					
p	6	6	6	variable				
q	4	4	4	4				
α	7	7	7	7				
iter_{max}	100	100	200	100				
$\varepsilon_{\text{PE, s, h, corr}}$	2^{-32}	2^{-32}	2^{-32}	2^{-32}				
μ	≈ 20.15	≈ 20.15	24	variable				

TABLE IV: On the left we list the input parameters for the simulations. On the right, we show the chosen reconciliation efficiency β for each SNR, together with the respective rate R_{code} and the row weight d_c of the LDPC code.

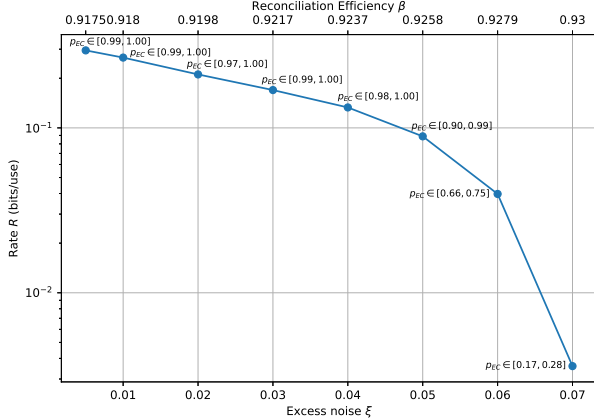


FIG. 5: Composable secret key rate R (bits/use) versus the excess noise ξ . The values of the reconciliation efficiency β are shown on the top axis and are chosen so as to produce $R_{\text{code}} = 0.9$. Every point represents the average value of R , which is obtained by 6 simulations. Other parameters are taken as in Table IV.

ter composable rate than the other choice ($\beta = 0.9075$) in correspondence of the same SNR, as shown in Fig. 7.

The spike in Fig. 6 follows the rule of the general trade-off between reconciliation efficiency and FER. Higher β means less amount of leaked information to the eavesdropper for each block. At the same time, less information is exchanged between the parties for correcting the given block resulting in a higher probability for this block to fail EC, i.e., higher value for the FER.

Fig. 7 shows the composable key rate R versus SNR for different discretization values p , while keeping the value of q the same (see list of parameters in Table IV). As observed, for fixed values of SNR and β , the lower the p is,

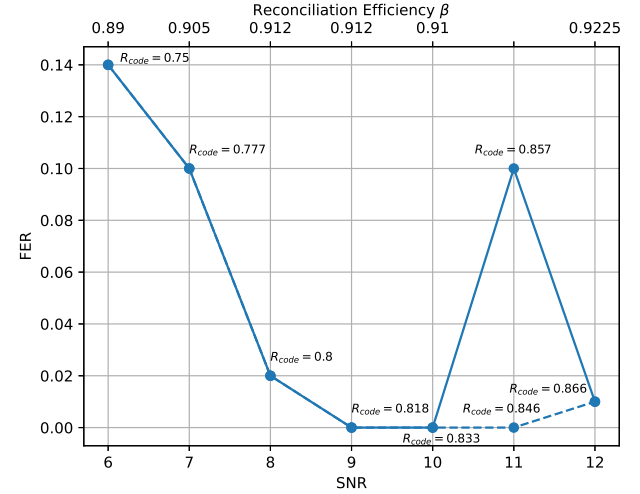


FIG. 6: FER versus SNR for $p = 6$. The maximum number of EC iterations is $\text{iter}_{\text{max}} = 100$. The reconciliation efficiency β is shown on the top axis while the respective value of R_{code} is displayed next to the points. The other parameters are constant and listed in Table IV. For SNR = 11, we show the points for $\beta = 0.932$ (solid line) and $\beta = 0.9075$ (dashed line), with the corresponding R_{code} depicted on top of the points.

the higher the rate R is. For every SNR and β , there is a maximum value for p able to achieve a positive R . For example, for SNR = 6 and $\beta = 0.89$, a positive R is impossible to achieve with $p \geq 7$. For SNR = 8 and $\beta = 0.912$, a positive R is infeasible with $p \geq 8$. The improvement based on a smaller p relies on the fact that a smaller amount of bits $d = p - q$ are declared publicly, while the protocol maintains a good EC performance thanks to a sufficiently large number of EC iterations.

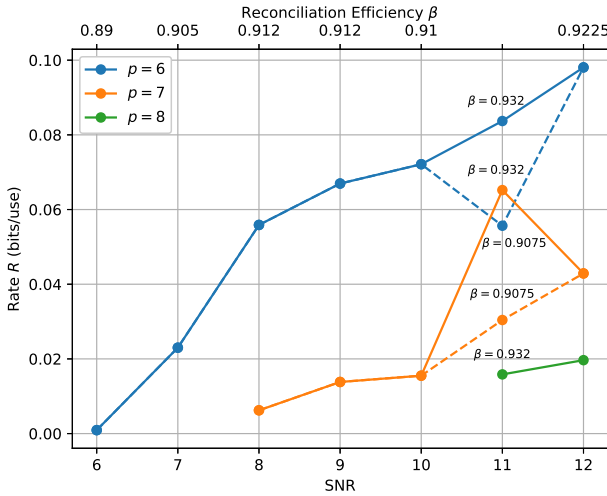


FIG. 7: Composable secret key rate R versus SNR for discretization bits $p = 6$, $p = 7$ and $p = 8$. The reconciliation efficiency β , chosen for each value of SNR, is shown on the top axis. For SNR = 11, the values of β are marked next to the points. We observe that, for lower values of p (at fixed q), we obtain higher rates. Other parameters are chosen as in Table IV.

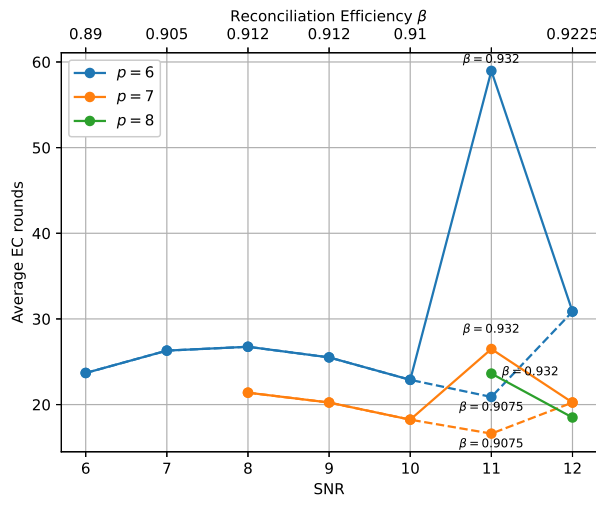


FIG. 8: Average EC rounds fnd_{rnd} needed to decode a frame versus SNR, for $p = 6$, $p = 7$ and $p = 8$. A round is registered only if the frame passes the verification step. The reconciliation efficiency β for each SNR is shown on the top axis. For SNR = 11, the values of β are marked next to the points. Other parameters are chosen as in Table IV.

On the other hand, it is clear that, by increasing p for fixed q , we increase the number d of public bits assisting the LDPC decoding via the sum-product algorithm. This means that the EC step is successfully terminated in a fewer rounds. In Fig. 8, we plot the average number of EC rounds fnd_{rnd} required to decode a block versus the SNR, for different values of p . For a larger value of

p , fewer decoding rounds are needed. This does not only make the decoding faster, but, depending on the specified $iter_{max}$, it also gives the algorithm the ability to achieve a lower FER. Thus, a higher p can potentially achieve a better p_{EC} , while a smaller p may return a better R (assuming that $iter_{max}$ is large enough). Therefore, at any fixed SNR and $iter_{max}$, one could suitably optimize the protocol over the number of discretization bits p .

V. CONCLUSIONS

In this manuscript we have provided a complete procedure for the processing of data as generated by a numerical simulation (or an equivalent experimental implementation) of a CV-QKD protocol. The procedure goes into the details of the various steps of parameter estimation, error correction and privacy amplification, suitably adapted to match the setting of composable finite-size security. Together with the development of the theoretical tools, and the corresponding technical details, we provide a complete Python library that can be used for CV-QKD simulation/optimization and for the complete data processing of CV-QKD experimental data.

Appendix A: Alternative formulas for PE

Here we present another way for applying the PE step, which follows Ref. [30]. Using m instances x_i and y_i of Alice's and Bob's random variables, we write

$$\widehat{T} = \frac{1}{\eta^2 \sigma_x^4} \left(\widehat{C}_{xy} \right)^2, \quad (A1)$$

where

$$C_{xy} = \sqrt{\eta T} \sigma_x^2 \quad (A2)$$

is the covariance of x and y . Its estimator can be computed as follows

$$\widehat{C}_{xy} = \frac{1}{m} \sum_{i=1}^m x_i y_i, \quad (A3)$$

which is normally distributed with mean equal to C_{xy} and variance

$$V_{C_{xy}} = \frac{1}{m} (2\eta T \sigma_x^4 + \sigma_x^2 \sigma_z^2). \quad (A4)$$

Then we express \widehat{T} as a (scaled) non-central chi-squared variable

$$\widehat{T} = \frac{V_{C_{xy}}}{\eta^2 \sigma_x^4} \left(\frac{\widehat{C}_{xy}}{\sqrt{V_{C_{xy}}}} \right)^2, \quad (A5)$$

since $\widehat{C}_{xy}/\sqrt{V_{C_{xy}}}$ follows a standard normal distribution. Then the mean and variance of \widehat{T} is given by the associated non-central chi-squared parameters $k = 1$ and

$\lambda = \frac{C_{xy}^2}{V_{C_{xy}}}$. Therefore, we obtain

$$\mathbb{E}(\hat{T}) = \frac{V_{C_{xy}}}{\eta^2 \sigma_x^4} \left(1 + \frac{C_{xy}^2}{V_{C_{xy}}} \right), \quad (\text{A6})$$

and

$$\text{Var}(\hat{T}) = \frac{2V_{C_{xy}}^2}{\eta^4 \sigma_x^8} \left(1 + 2 \frac{C_{xy}^2}{V_{C_{xy}}} \right). \quad (\text{A7})$$

Using Eqs. (A2) and (A4), and keeping only the significant terms with respect to $1/m$, we have

$$\mathbb{E}(\hat{T}) = T, \quad \text{Var}(\hat{T}) = \frac{4}{m} T^2 \left(2 + \frac{\sigma_z^2}{\eta T \sigma_x^2} \right) := \sigma_T^2. \quad (\text{A8})$$

The estimator for the noise variance σ_z^2 is given by

$$\widehat{\sigma_z^2} = \frac{1}{m} \sum_{i=1}^m \left(y_i - \sqrt{\eta \hat{T}} x_i \right)^2. \quad (\text{A9})$$

We then assume that $\hat{T} \approx T$ and rescale by $1/\sigma_z$ the term inside the brackets in the relation above, so as to have a standard normal distribution for the variable $\frac{y_i - \sqrt{\eta T} x_i}{\sigma_z}$. Thus, we obtain

$$\widehat{\sigma_z^2} = \frac{\sigma_z^2}{m} \sum_{i=1}^m \left(\frac{y_i - \sqrt{\eta T} x_i}{\sigma_z} \right)^2, \quad (\text{A10})$$

and observe that this is a (scaled) chi-squared variable. From the associated chi-squared parameters $k = m$ (and $\lambda = 0$), we calculate the following mean and variance

$$\mathbb{E}(\widehat{\sigma_z^2}) = \sigma_z^2, \quad (\text{A11})$$

$$\text{Var}(\widehat{\sigma_z^2}) = \frac{2\sigma_z^4}{m}. \quad (\text{A12})$$

Then, from the formula

$$\sigma_z = 1 + v_{\text{el}} + \Xi, \quad (\text{A13})$$

we have that

$$\mathbb{E}(\widehat{\Xi}) = \Xi, \quad (\text{A14})$$

$$\text{Var}(\widehat{\Xi}) = \frac{2\sigma_z^4}{m} := \sigma_{\Xi}^2. \quad (\text{A15})$$

The worst-case estimators will be given by

$$T_m = T - w\sigma_T, \quad \Xi_m = \Xi + w\sigma_{\Xi}. \quad (\text{A16})$$

Appendix B: LDPC decoding

1. Updating the Likelihood function

Let us assume a device where its output is described by the random variable X taking values $x \in \mathcal{X}$ according to a family of probability distributions $\mathcal{P}(X; \theta)$

$$\mathbf{H} = \begin{bmatrix} 0 & 0 & 3 & 0 & 1 \\ 2 & 0 & 0 & 1 & 0 \\ 0 & 1 & 0 & 2 & 3 \end{bmatrix}$$

TABLE V: An example for a $l \times n$ parity check matrix with values in $\mathcal{GF}(2^2)$ for $l = 3$ checks (check nodes) and $n = 5$ transmitted signals (variable nodes). For this matrix, the assumptions of a regular code explained in Sec. IID are not valid and it is used only as a toy model for the convenience of the description for the sum-product algorithm.

Algorithm 2 Non-Binary Sum-Product Algorithm

```

Input:  $P(\bar{K}_i | X_i \underline{K}_i)$ ,  $K_{\text{sd}}^l$ , Output:  $\hat{K}^n$ ,  $\text{fnd}$ ,  $\text{fnd}_{\text{rnd}}$ 
1: Step 1: Initialization
2:  $\bar{z} \leftarrow K_{\text{sd}}^l$ 
3:  $j, i \leftarrow j, i : \mathbf{H}_{ji} \neq 0$  (Tanner Graph creation)
4:  $f_i^{\bar{\kappa}} \leftarrow P(\bar{K}_i = \bar{\kappa} | X_i, \underline{K}_i)$ 
5:  $q_{j i \bar{\kappa}} \leftarrow f_i^{\bar{\kappa}}$ 
6: for  $\text{iter} = 1, 2, \dots, \text{iter}_{\text{max}}$  do
7:   Step 2: Horizontal Step
8:    $r_{j i \bar{\kappa}} \leftarrow \sum_{s: t: s+t=z_j - \mathbf{H}_{ji} \bar{\kappa}} \Pr \left[ \sigma_{j(i-1)} = s \right] \Pr \left[ \rho_{j(i+1)} = t \right]$ 
9:   Step 3: Vertical Step
10:   $q_{j i}^{\bar{\kappa}} \leftarrow \alpha_{ji} f_i^{\bar{\kappa}} \prod_{m \setminus j} r_{m i \bar{\kappa}}, \alpha_{ji} : \sum_{\bar{\kappa}=0}^{2^q-1} q_{j i \bar{\kappa}} = 1$ 
11:  Step 4: Tentative Decoding
12:   $\hat{K}_i \leftarrow \arg \max_{\bar{\kappa}} f_{i \bar{\kappa}} \prod_j r_{j i \bar{\kappa}}$ 
13:  if  $\mathbf{H} \hat{K}^n = \bar{z}$  then
14:    return  $\hat{K}^n, \text{fnd}_{\text{rnd}}, \text{fnd} \leftarrow \text{True}$ 
15:  end if
16:  if  $\text{iter} = \text{iter}_{\text{max}}$  then
17:    return  $\text{fnd} \leftarrow \text{False}$ 
18:  end if
19: end for

```

parametrized by θ . Given the sampled data string X_i for $i = 1, \dots, n$ from this distribution, one can build a string of data X^n and define the likelihood of a specific parameter θ describing the associated probability distribution as

$$\mathcal{L}(\theta | X^n) = P(X^n | \theta) = \prod_{i=1}^n P(X_i | \theta), \quad (\text{B1})$$

where $P(X^n | \theta)$ is the conditional probability for a specific X^n to come out of the device given that its distribution is described by θ and the its outcome of the device is i.i.d. following $\mathcal{P}(X; \theta)$. Intuitively, then a good guess $\hat{\theta}$ of the parameter θ would be the argument θ^* of the maximization of the likelihood function over θ . Using Baye's rule, we may write

$$P(X^n | \theta) = \frac{P(X^n)}{P(\theta)} P(\theta | X^n) \quad (\text{B2})$$

and observe that $P(X^n)$ is not dependent on θ and $P(\theta)$ is considered uniform (thus independent of θ). Therefore, one may maximize $P(\theta | X^n)$ instead. Furthermore,

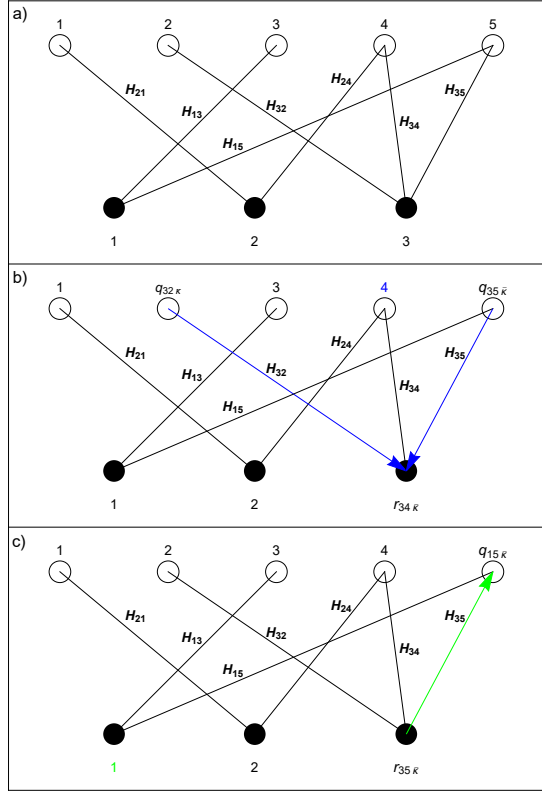


FIG. 9: a) Here is the Tanner graph of the parity check matrix of Table V. We see that the variable (output) nodes (white disks) are connected with the check (syndrome) nodes (black disks) when $\mathbf{H}_{ji} \neq 0$. b) One instance of the horizontal step (Step 2) of Algorithm 2. Here the signal probability $r_{34\bar{\kappa}}$ is updated for all the $\bar{\kappa} \in \mathcal{GF}(2^2)$ from the contribution (blue arrows) of the rest of the neighbour variable nodes of check node 3 apart from the variable node 4 (node in blue). This update will be repeated in the same step for all the variable nodes, i.e., $r_{32\bar{\kappa}}$ and $r_{35\bar{\kappa}}$ will be calculated too. The same procedure will be followed for syndrome nodes 1 and 2 before the algorithm passes to the horizontal step. Note that this previous description gives the conceptual steps to derive the desirable result. Practically, the algorithm follows a more complex path, e.g., calculates probabilities of partial sums. However, this path gives an advantage in terms of efficient calculations. c) An instance of the horizontal step (Step 3) of Algorithm 2. Here the probability $q_{15\bar{\kappa}}$ is updated for all the $\bar{\kappa} \in \mathcal{GF}(2^2)$. It is updated only from the contribution of syndrome node 3 (green arrow) while node 1 (node in green) is not participating. This update will happen for all the syndrome nodes, namely, $q_{35\bar{\kappa}}$ will be calculated too. It will be repeated also for all variable nodes before the tentative decoding (Step 4) is going to start.

for the simplification of the later discussion one may express the previous probability as a function being only dependent from the parameter θ (considering the data X_i as constants), namely

$$F(\theta) = P(\theta|X^n) \quad (B3)$$

Let us now consider the case where we have a vector

of parameters (variables) $\vec{\theta} = (\theta_1, \dots, \theta_n)$ describing the distribution $\mathcal{P}(X|\theta)$. Respectively, one can define the probability

$$F(\vec{\theta}) = F(\theta_1, \dots, \theta_n) \quad (B4)$$

and its marginals

$$F(\theta_i) = \sum_{k \neq i} F(\theta_1, \dots, \theta_k, \dots, \theta_n). \quad (B5)$$

Let us now assume that there are certain constraints that $\vec{\theta}$ should satisfy which are summarized by a system of m linear equations (checks) $\mathbf{H}\vec{\theta} = \vec{z}$, where \mathbf{H} is an $m \times n$ matrix. In particular, there are m equations that the θ_i should satisfy in the form of

$$\sum_i \mathbf{H}_{ji} \theta_i = z_j \quad \text{for } j = 1, \dots, m \quad (B6)$$

For instance, when $\vec{z} = (3, 1, 2)$, the matrix in Table V gives the following three equations [39]:

$$3\theta_3 + \theta_5 = 3 \quad (B7)$$

$$2\theta_1 + \theta_4 = 1 \quad (B8)$$

$$\theta_2 + 2\theta_4 + 3\theta_5 = 2 \quad (B9)$$

Then one needs to pass from the (a-priori) probability distribution of equation Eq. (B4) to

$$\tilde{F}(\vec{\theta}) = F(\vec{\theta}|\mathbf{H}\vec{\theta} = \vec{z}) \quad (B10)$$

and calculate the respective marginals

$$\tilde{F}(\theta_i) = F(\theta_i|\mathbf{H}\vec{\theta} = \vec{z}). \quad (B11)$$

2. Sum-product Algorithm

The sum product algorithm uses the intuition of the previous analysis to calculate efficiently the marginals

$$\tilde{F}(\overline{K}_i) = F(\overline{K}_i|\mathbf{H}\overline{K}^n = K_{sd}^l) \quad (B12)$$

of Eq. (B11) for $\theta_i := \overline{K}_i$, $\vec{\theta} := \overline{K}^n$, $\vec{z} := K_{sd}^l$ and *a priori* marginal probabilities $F(\overline{K}_i = \bar{\kappa}) = P(\bar{\kappa}|X_i \overline{K}_i)$ (calculated in Eq. 54). To do so, it associates a Tanner (factor) graph to the matrix \mathbf{H} and assumes signal exchange between its nodes. More specifically, the graph consist of two kinds of nodes: n variable nodes representing the parameters (variables) \overline{K}_i and m check nodes representing the linear equations (checks) described by $\mathbf{H}\overline{K}^n = K_{sd}^l$. Then for each variable i that participates in the j th equation there is an edge connecting the relevant nodes. At this point, we present an example of such a factor graph (otherwise Tanner graph, especially when it is associated with the parity check matrix of an LDPC) in Fig. 9(a) based on the matrix \mathbf{H} in Table V. The signal sent from the variable node i to a factor node j is called $q_{ji\bar{\kappa}}$ and

is the probability that the variable $\bar{K}_i = \bar{\kappa}$ and all the linear equations are true apart from equation j . The signal sent from the check node j to the variable node i is called $r_{j\bar{\kappa}}$ and is equal with the probability of equation j to be satisfied if the variable $\bar{K}_i = \bar{\kappa}$. Note that, based on this definitions, the marginals of Eq. (B12) are given by

$$\tilde{F}(\bar{K}_i = \bar{\kappa}) = q_{j\bar{\kappa}} r_{j\bar{\kappa}} \quad (\text{B13})$$

for any equation j that the variable i takes part in.

In particular, in each iteration the algorithm updates the $r_{j\bar{\kappa}}$ (horizontal step) through the signals of the neighbour variable nodes apart from the signal from node i by the following rule: given a vector \bar{K}^n where its i th element is equal to $\bar{K}_i = \bar{\kappa}$ we have

$$r_{j\bar{\kappa}} = \sum_{\{i\}} \text{Prob}[K_{\text{sd}j} | \bar{K}^n] \prod_{k \in \mathcal{N}(j) \setminus i} q_{jk\bar{K}_k}, \quad (\text{B14})$$

where $\text{Prob}[K_{\text{sd}j} | \bar{K}^n]$ takes values 1 or 0 whether the check j is satisfied from \bar{K}^n or not. Note that the values of $q_{jk\bar{K}_k}$ are initially updated with the *a priori* probabilities during the initialization step (see line 5 of Algorithm 2) and that $\mathcal{N}(j)$ are the set of neighbours of the j th check node. An example of such an update is depicted in Fig. 9(b).

In fact, the algorithm takes advantage of the fact that

$$r_{j\bar{\kappa}} = \text{Prob} [\sigma_{j(i-1)} + \rho_{j(i+1)} = K_{\text{sd}j} - \mathbf{H}_{ji} \bar{K}_i] \quad (\text{B15})$$

where

$$\sigma_{jk} = \sum_{i: i \leq k} \mathbf{H}_{ji} \bar{K}_i \quad (\text{B16})$$

$$\rho_{jk} = \sum_{i: i \geq k} \mathbf{H}_{ji} \bar{K}_i \quad (\text{B17})$$

are partial sums with different direction running over the j th check. More specifically, Eq. (B15) can be further simplified into a sum of a product of probabilities of the previous partial sums taking specific values by satisfying the j th check as in line 10 of the pseudo-code of Algorithm 2. Then the algorithm updates the $q_{j\bar{\kappa}}$ through the signals coming from the neighbour check nodes apart from node j (as depicted for the example in Fig. 9(c)). The rule to do so is given in line 12 of the pseudo-code (vertical step). Finally, in the tentative decoding step, the algorithm takes the product of $q_{j\bar{\kappa}}$ and $r_{j\bar{\kappa}}$, calculates and maximizes the marginal of Eq. (B13) over $\bar{\kappa}$. The arguments \hat{K}_i of this maximization of every marginal create a good guess \hat{K}^n for \bar{K}^n . In the next iteration the algorithm follows the same steps but know is using the previous $q_{j\bar{\kappa}}$ to make all the updates.

Appendix C: Calculations in $\mathcal{GF}(q)$

A Galois field is a field with finite number of elements. A common way to derive it is to take the modulo of the

division of the integers over a prime number p . The order of such a field $q = p^k$ (with k being a positive integer) is the number of its elements. All the Galois fields with the same number of elements are isomorphic and can be identified by $\mathcal{GF}(q)$. A special case is the order $q = 2^k$. In a field with such an order, each element is associated with a binary polynomial of degree no more than $k-1$, i.e. the elements can be described as k -bit strings where each bit of the string corresponds to the coefficient of the polynomial at the same position. For instance, for the element 5 of $\mathcal{GF}(2^3)$ we have

$$101 \rightarrow x^2 + 1.$$

This is instructive on how the operations of addition and multiplication are computed in such a field. For example the addition of 5 and 6 is made in the following way

$$101 + 110 \rightarrow (x^2 + 1) + (x^2 + x) = \underbrace{(1+1)x^2 + x + 1}_{011 \rightarrow 3}.$$

One can also perform the addition using a precomputed matrix (e.g., as generated by the Matlab library). For instance, for $\mathcal{GF}(2^3)$, we have

$$\mathbf{A} = \begin{pmatrix} 0 & 1 & 2 & 3 & 4 & 5 & 6 & 7 \\ 1 & 0 & 3 & 2 & 5 & 4 & 7 & 6 \\ 2 & 3 & 0 & 1 & 6 & 7 & 4 & 5 \\ 3 & 2 & 1 & 0 & 7 & 6 & 5 & 4 \\ 4 & 5 & 6 & 7 & 0 & 1 & 2 & 3 \\ 5 & 4 & 7 & 6 & 1 & 0 & 3 & 2 \\ 6 & 7 & 4 & 5 & 2 & 3 & 0 & 1 \\ 7 & 6 & 5 & 4 & 3 & 2 & 1 & 0 \end{pmatrix}. \quad (\text{C1})$$

The subtraction between two elements of $\mathcal{GF}(2^k)$ gives the same result as addition making the two operations equivalent. The multiplication is more complicated especially when the result is a polynomial with a degree larger than $k-1$. For example, in $\mathcal{GF}(2^3)$, 7×6 is calculated as

$$111 \times 110 \rightarrow (x^2 + x + 1) \times (x^2 + x) \\ = x^4 + x^3 + x^3 + x^2 + x^2 + x = x^4 + x. \quad (\text{C2})$$

Because we have a degree 4 polynomial, we need to take this result modulo an irreducible polynomial of degree 3, e.g., $x^3 - x + 1$. Thus, we have

$$(x^4 + x \bmod x^3 - x + 1) = x^2 \rightarrow 100 \rightarrow 4, \quad (\text{C3})$$

where the operation can be made by adopting a long division with exclusive OR [32]. As for the addition, one can perform the multiplication by using a pre-calculated matrix. For instance, in $\mathcal{GF}(2^3)$, the results are specified

by the following matrix

$$\mathbf{M} = \begin{pmatrix} 0 & 0 & 0 & 0 & 0 & 0 & 0 & 0 \\ 0 & 1 & 2 & 3 & 4 & 5 & 6 & 7 \\ 0 & 2 & 4 & 6 & 3 & 1 & 7 & 5 \\ 0 & 3 & 6 & 5 & 7 & 4 & 1 & 2 \\ 0 & 4 & 3 & 7 & 6 & 2 & 5 & 1 \\ 0 & 5 & 1 & 4 & 2 & 7 & 3 & 6 \\ 0 & 6 & 7 & 1 & 5 & 3 & 2 & 4 \\ 0 & 7 & 5 & 2 & 1 & 6 & 4 & 3 \end{pmatrix}. \quad (\text{C4})$$

Appendix D: Toeplitz matrix calculation with Fast-Fourier Transform

The time complexity of the dot product between a Toeplitz matrix \mathbf{T} and a sequence \mathbf{x} is $O(\tilde{n}^2)$. This complexity can be reduced to $O(\tilde{n} \log \tilde{n})$ using the definition of a circulant matrix and the fast Fourier transform. A circulant matrix \mathbf{C} is a special case of the Toeplitz matrix, where every row of the matrix is a right cyclic shift of the row above it [33]. Such a matrix is always square and is completely defined by its first row \mathbf{C}_{def} .

The steps are as follows [34]:

- The Toeplitz matrix is reformed into a circulant matrix by merging its first row and column to-

gether. Since the former has dimensions $\tilde{n} \times r$, where \tilde{n} is the privacy amplification block length and r is the length of the final key, the length of the definition of the latter becomes $\tilde{n} + r - 1$.

- The decoded sequence to be compressed is extended, as $r - 1$ zeros are padded to its end. The length of the new sequence \mathbf{S}_{ext} is now equal to the length of the circulant matrix definition.
- To efficiently calculate the key, an optimized multiplication is carried out as

$$\mathfrak{F}^{-1}[\mathfrak{F}(\mathbf{S}_{\text{ext}}) * \mathfrak{F}(\mathbf{C}_{\text{def}})] \quad (\text{D1})$$

where \mathfrak{F} represents the fast Fourier transform and \mathfrak{F}^{-1} stands for the inverse fast Fourier transform. Because of the convolution theorem, the $*$ operator signifies the Hadamard product and therefore element-wise multiplication can be performed.

- As the key format is required to be in bits, the result of the inverse fast Fourier transform is taken modulo 2.
- The key \mathbf{K} is constituted by the first r bits of the resulting bit string of length $\tilde{n} + r - 1$.

[1] S. Pirandola, U. L. Andersen, L. Banchi, M. Berta, D. Bunandar, R. Colbeck, D. Englund, T. Gehring, C. Lupo, C. Ottaviani, J. L Pereira, M. Razavi, J. S. Shaari, M. Tomamichel, V. C. Usenko, G. Vallone, P. Villoresi, and P. Wallden, “Advances in quantum cryptography,” *Adv. Opt. Photon.* **12**, 1012–1236 (2020).

[2] C. H. Bennett and G. Brassard, “Quantum cryptography: public key distribution and coin tossing,” in *Proceedings of the International Conference on Computers, Systems & Signal Processing*, Bangalore, India, December 1984, pp. 175–179.

[3] D. Bunandar, L. C. G. Govia, H. Krovi, and D. Englund, “Numerical finite-key analysis of quantum key distribution,” *npj Quantum Inf.* **6**, 104 (2020).

[4] F. Grosshans and P. Grangier, “Continuous variable quantum cryptography using coherent states,” *Phys. Rev. Lett.* **88**, 057902 (2002).

[5] C. Weedbrook, A. M. Lance, W. P. Bowen, T. Symul, T. C. Ralph, P. K. Lam, “Quantum cryptography without switching,” *Phys. Rev. Lett.* **93**, 170504 (2004).

[6] C. Weedbrook, S. Pirandola, R. García-Patrón, N. J. Cerf, T. C. Ralph, J. H. Shapiro, and S. Lloyd, “Gaussian quantum information,” *Rev. Mod. Phys.* **84**, 621 (2012).

[7] S. Pirandola, R. Laurenza, C. Ottaviani, and L. Banchi, “Fundamental Limits of Repeaterless Quantum Communications,” *Nat. Commun.* **8**, 15043 (2017).

[8] S. Pirandola, C. Ottaviani, G. Spedalieri, C. Weedbrook, S. L. Braunstein, S. Lloyd, T. Gehring, C. S. Jacobsen, and U. L Andersen, “High-rate measurement-device- independent quantum cryptography,” *Nat. Photon.* **9**, 397–402 (2015).

[9] Y. Zhang, Z. Chen, S. Pirandola, X. Wang, C. Zhou, B. Chu, Y. Zhao, B. Xu, S. Yu, and H. Guo, “Long-Distance Continuous-Variable Quantum Key Distribution over 202.81 km of Fiber,” *Phys. Rev. Lett.* **125**, 010502 (2020).

[10] C. Zhou, X. Wang, Y. Zhang, Z. Zhang, S. Yu, and H. Guo, “Continuous-Variable Quantum Key Distribution with Rateless Reconciliation Protocol,” *Phys. Rev. Applied* **12**, 054013 (2019).

[11] The CVQKDsim library is freely available on github at: <https://github.com/alex-moodi/CVQKDsim>

[12] S. Pirandola, “Limits and Security of Free-Space Quantum Communications,” *Phys. Rev. Research* **3**, 013279 (2021).

[13] D. J. C. Mackay, “Good error-correcting codes based on very sparse matrices,” *IEEE Trans. Inform. Theory* **45**, 399–431 (1999).

[14] M. C. Davey and D. MacKay, “Low-density parity check codes over $GF(q)$,” *IEEE Communications Letters* **2**, 165–167 (1998).

[15] D. Huang, D. Lin, C. Wang, W. Liu, S. Fang, J. Peng, P. Huang, and G. Zeng, “Continuous-variable quantum key distribution with 1 mbps secure key rate,” *Opt. Express* **23**, 17511–17519 (2015).

[16] D. K. Lin, D. Huang, P. Huang, J. Y. Peng, and G. H. Zeng, “High performance reconciliation for continuous-variable quantum key distribution with LDPC code,” *Int.*

J. Quantum Inform. **13**, 1550010 (2015).

[17] C. Pacher, J. Martinez-Mateo, J. Duhme, T. Gehring, and F. Furrer, “Information Reconciliation for Continuous-Variable Quantum Key Distribution using Non-Binary Low-Density Parity-Check Codes,” [arXiv:1602.09140](https://arxiv.org/abs/1602.09140)

[18] F. R. Kschischang, B. J. Frey, and H. Andrea Loeliger, “factor graphs and the sum-product algorithm,” IEEE Trans. Inform. Theory **47**, 498–519 (2001).

[19] M. Milisevic, “Low-Density Parity-Check Decoder Architectures for Integrated Circuits and Quantum Cryptography,” (PhD thesis, University of Toronto, 2017).

[20] T. Tsurumaru and M. Hayashi, “Dual universality of hash functions and its applications to quantum cryptography,” IEEE Trans. Info. Theory **59**, 4700–4717 (2013)

[21] Q. Li, B.-Z. Yan, H.-K. Mao, and X.-F. Xue, “High-speed implementation of fft-based privacy amplification on fpga in quantum key distribution,” [arXiv:1809.07592](https://arxiv.org/abs/1809.07592).

[22] S. Pirandola, S. L. Braunstein, and S. Lloyd, “Characterization of Collective Gaussian Attacks and Security of Coherent-State Quantum Cryptography,” Phys. Rev. Lett. **101**, 200504 (2008).

[23] T. M Cover and J. A. Thomas, “Elements of information theory,” (Wiley, 2012).

[24] D. S. Slepian and J. K. Wolf, “Noiseless Coding of Correlated Information Sources”, IEEE Trans. Inf. Theory **19**, 471–480 (1973).

[25] A. D. Wyner, “Recent results in Shannon theory,” IEEE Trans. Inform. Theory **20**, 2-10 (1974).

[26] P. Papanastasiou, C. Weedbrook, and S. Pirandola, “Continuous-variable quantum key distribution in fast fading channels,” Phys. Rev. A **97**, 032311 (2018).

[27] D. J. C. MacKay, and R. M. Neal, “Near Shannon limit performance of low density parity check codes,” Elect. Lett. **33**, 457-458 (1997).

[28] M. Thorup, “High Speed Hashing for Integers and String,” [arXiv:1504.06804](https://arxiv.org/abs/1504.06804)v9.

[29] Note that α and q also affect the *a-priori* probabilities of the decoding step in Eqs. (54) and (55) which, in turn, affect the p_{EC} for a given number of maximum iterations $iter_{max}$.

[30] L. Ruppert, V. C. Usenko, and R. Filip, “Long-distance continuous-variable quantum key distribution with efficient channel estimation”, Phys. Rev. A **90**, 062310 (2014).

[31] F. R. Kschischang, B. J. Frey, and H. -A. Loeliger, “Factor Graphs and the Sum-Product Algorithm,” IEEE Trans. Inform. Theory **47**, 498 (2001).

[32] G. L. Mullen and D. Panario, “Handbook of Finite Fields,” (CRC Press, 2013).

[33] R. M. Gray, “Toeplitz and Circulant Matrices: A Review,” Foundations and Trends in Communications and Information Theory **2**, 155–239 (2006).

[34] B. Tang, B. Liu, Y. Zhai, C. Wu, and W. Yu, “High-speed and Large-scale Privacy Amplification Scheme for Quantum Key Distribution”, Sci. Rep. **9**, 15733 (2019).

[35] For instance see: Dmitry Panchenko, 18.650 Statistics for Applications, Fall 2006, MIT.

[36] A. Leverrier, F. Grosshans, and P. Grangier, Phys. Rev. A **81**, 062343 (2010).

[37] That is true for the MLES for τ_A and τ_B because Alice modulates her mode independently from Bob. Then from the theory of linear multiple regression this is true between the group of τ_{Aq} and τ_{Bq} and the MLE for σ_z^2 . The same reasoning holds for $\widehat{\tau}_{A_p}$, $\widehat{\tau}_{B_p}$ and $\sigma_{z'}^2$.

[38] We assume here an extra step before PE: Alice and Bob multiply their measurements with 2.

[39] Note that these equations are valid in $\mathcal{GF}(4)$

[40] S. Pirandola, C. Ottaviani, G. Spedalieri, C. Weedbrook, S. L. Braunstein, S. Lloyd, T. Gehring, C. S. Jacobsen, and U. L. Andersen, “High-rate measurement-device-independent quantum cryptography”, Nat. Phot. **9**, 397–402(2015).